TECHNISCHE UNIVERSITÄT WIEN

LDA+DMFT approach to calculation of RIXS spectra

Jan Kuneš

Institute of Solid State Physics, TU Wien

Collaborators

Sponsored by

Atsushi Hariki

Mathias Winder

Takayuki Uozumi
(OPU, Japan)

LDA+DMFT approach to core-level spectroscopy

A. Hariki, T. Uozumi and JK, Phys. Rev. B **96**, 045111 (2017)

LDA+DMFT study of L-edge RIXS in high-valence cuprates

A. Hariki, M. Winder and JK, Phys. Rev. Lett. **122**, 126403 (2018)

Resonant inelastic X-ray scattering (RIXS)

Resonant inelastic X-ray scattering : Powerful probe with broad sensitivity to **two-particle excitations** of charge, orbital, spin and lattice degrees of freedom

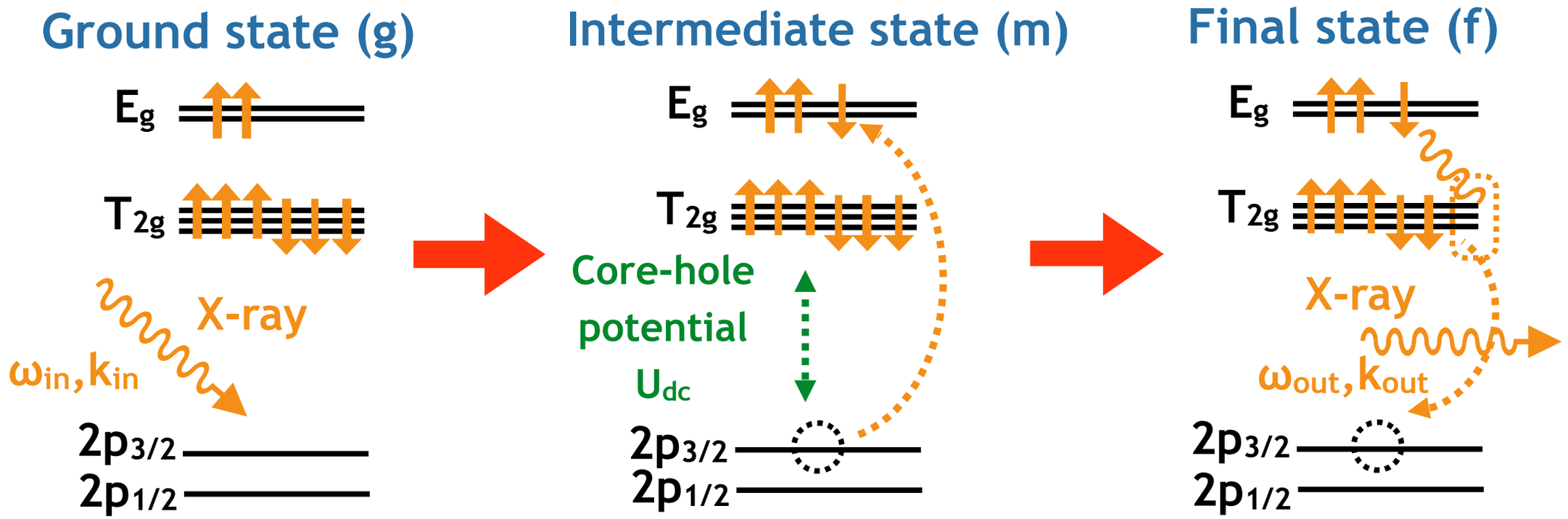

$$F_{\mathrm{RIXS}}(\omega_{\mathrm{in}},\omega_{\mathrm{out}}) = \sum_f \Big| \sum_m \frac{\langle f|V_E|m\rangle\langle m|V_I|g\rangle}{\omega_{\mathrm{in}}+E_g-E_m+i\Gamma}\Big|^2 \delta(\omega_{\mathrm{in}}+E_g-\omega_{\mathrm{out}}-E_f)$$

$$= -\frac{1}{\pi}\mathrm{Im}\ \langle g|R^\dagger(\boldsymbol{q},\omega_{\mathrm{in}})\ \frac{1}{\omega_{\mathrm{loss}}+E_g-H+i\delta}\ R(\boldsymbol{q},\omega_{\mathrm{in}})|g\rangle$$

Propagation on lattice

X-ray absorption-emission

$$R(\boldsymbol{q},\omega_{\mathrm{in}}) = V_E \frac{1}{\omega_{\mathrm{in}}+E_g-H+i\Gamma} V_I$$

H with **core–hole**

M. W. Haverkort, PRL **105**, 167404 (2010)

Theoretical modeling of RIXS in correlated materials

1. Atomic limit

Valence-valence and core-valence interaction

no lattice (=no dispersion)

cluster **multicluster**

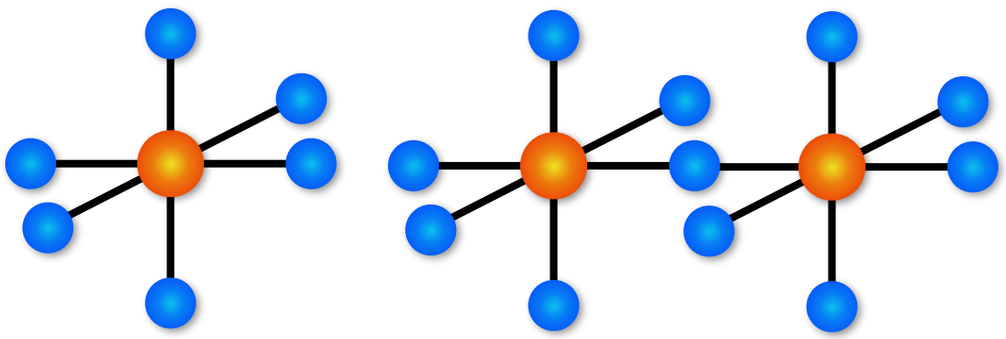

ab-initio cluster model (and beyond)

M. W. Haverkort et al. PRB **85**, 165113 (2012)
J. Luder et al. PRB **96**, 245131 (2017)

Multisite extension
- **computationally expensive**
- **more tuning parameters …**

Recent development with DMRG etc.

A. Nocera et al. Sci. Rep. **8**, 11080 (2018)
T. Toyama et al., PRB **92**, 014515 (2015)

2. Noninteracting limit

Material-specific band structure

approx. electron-hole interaction

e.g. Bethe-Salpeter approach

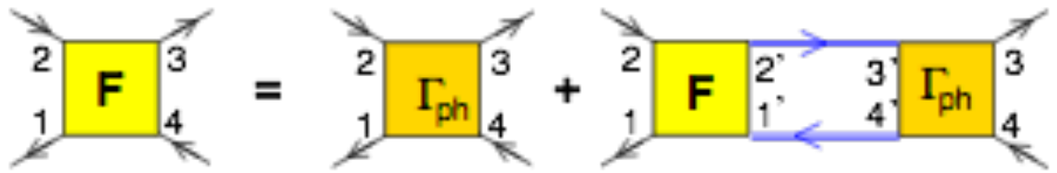

J. Vinson et al. PRB **83**, 115106 (2011)
K. Gilmore et al. Comput. Phys. Commun. **197**, 109 (2015)
T. Nomura. J. Phys. Soc. Jpn. **84**, 094704 (2015)

Crude approximation on many-body effect in both ground and excited states

Merge advantages in the two approaches together ?
= ultimate goal of theoretical modeling

LDA+DMFT approach to RIXS in correlated materials

Local density approximation (LDA) + Dynamical mean-field theory (DMFT)

successful ab-initio many-body scheme in describing electronic properties of correlated materials

Ref. A. Georges et al., RMP **68**, 13 (1996) / G. Kotliar et al., RMP **78**, 865 (2006)

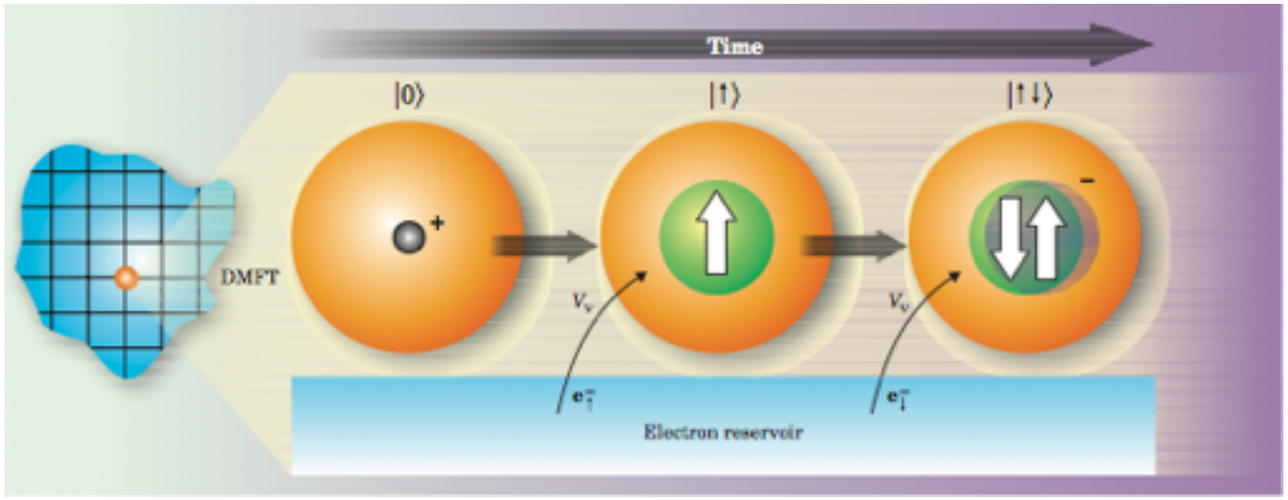

Material specific bands : LDA
(multi-band Hubbard model)
+
Local electron correlation : DMFT
= Many-body dynamics in realistic materials

$$\Delta(i\omega_n) = -G^{-1}(i\omega_n) + i\omega_n - h^{\mathrm{local}} - \Sigma(i\omega_n)$$

: hybridization intensity

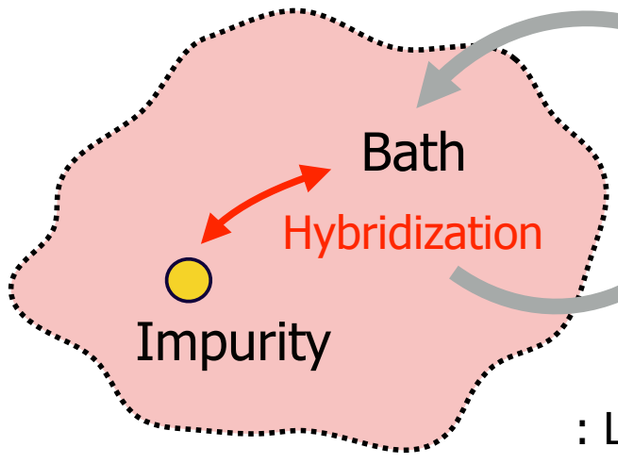

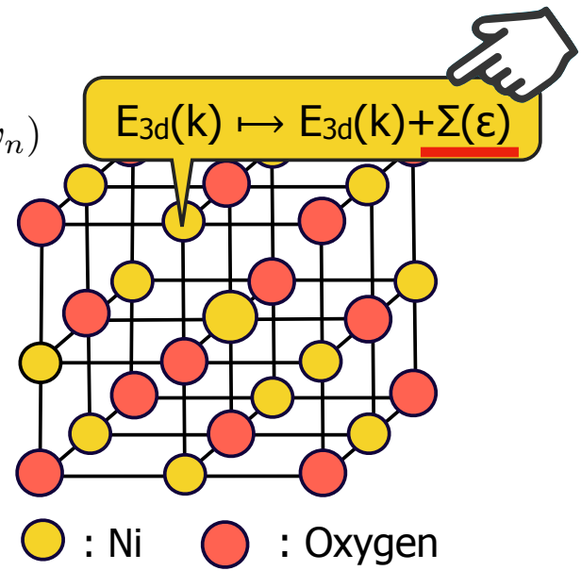

$$\Sigma(i\omega_n) = G_0^{-1}(i\omega_n) - G(i\omega_n)^{-1}$$

: Local self-energy (dynamical M.F.)

LDA+DMFT: 1P spectra

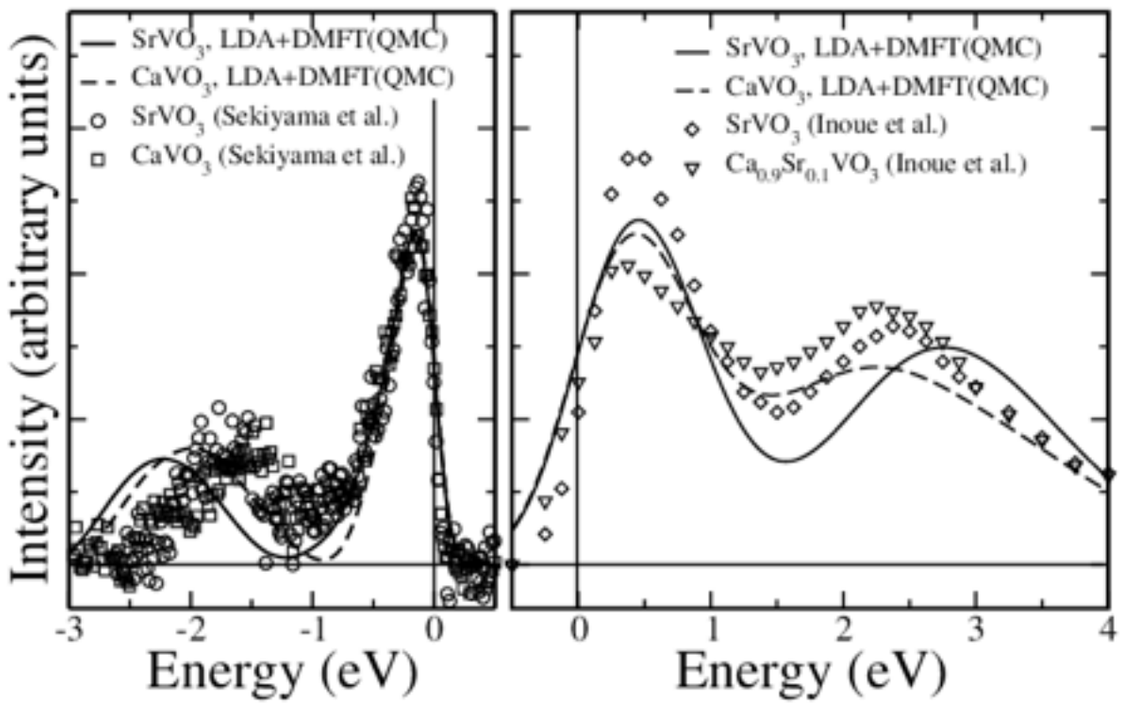

*I. Nekrasov et al., PRB **72**, 155106 (2005)*

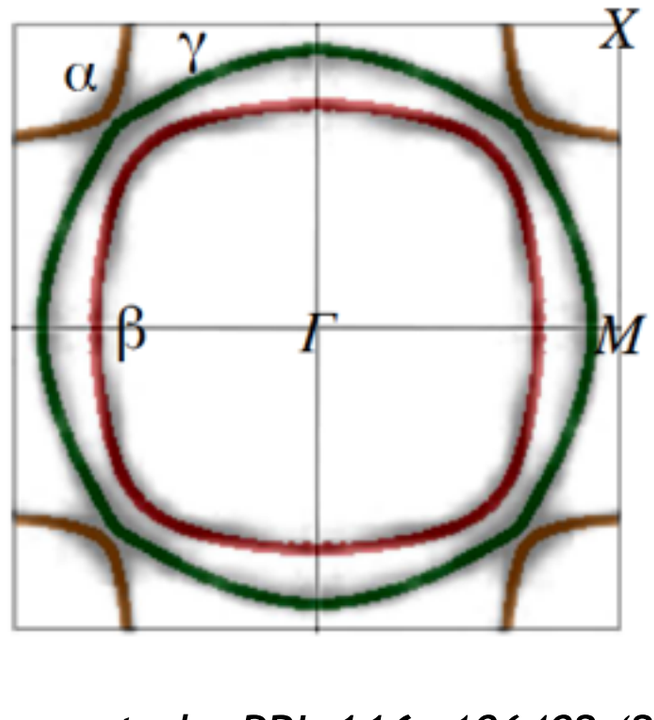

*G. Zhang et al., PRL **116**, 106402 (2016)*

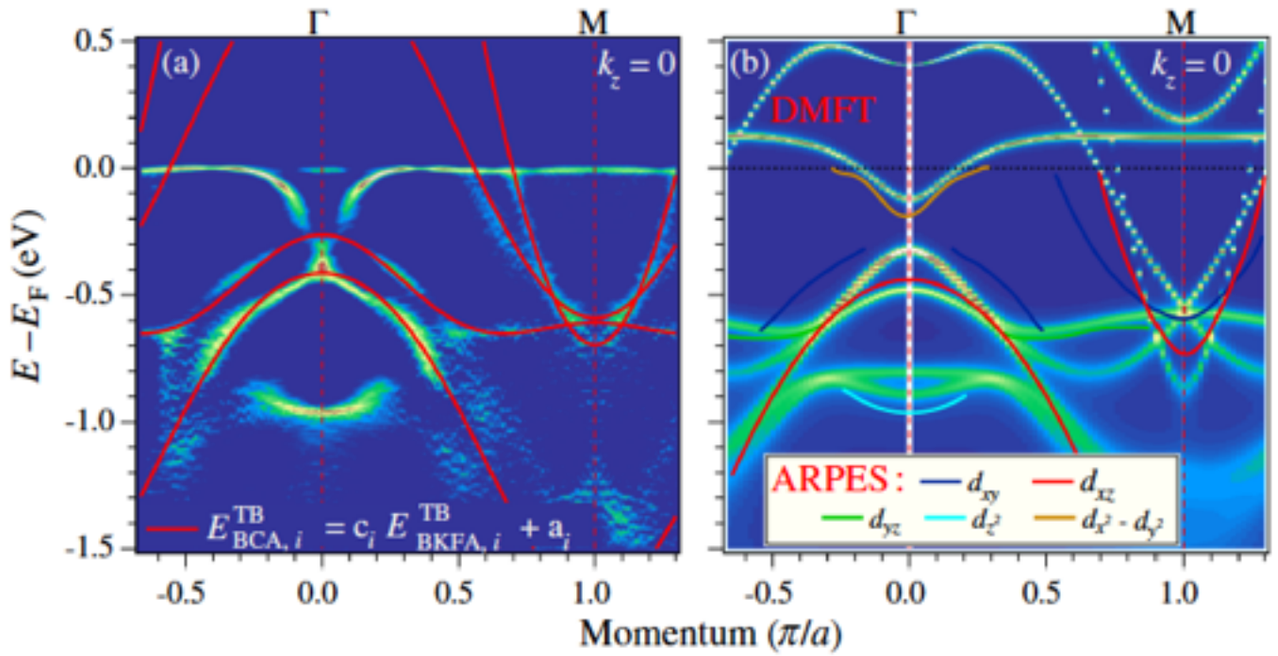

*N. Xu et al., PRX **3**, 011006 (2013)*

LDA+DMFT: 2P spectra (limited)

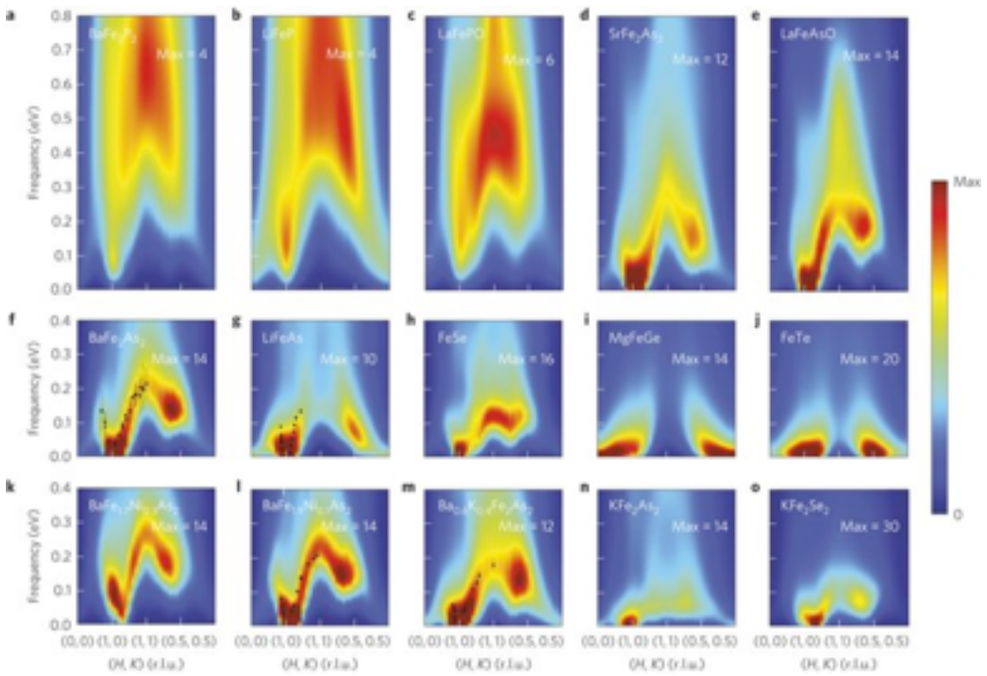

iron pnictides
multi-orbital,
modified RPA treatment

Z. P. Yin, K. Haule and G. Kotliar, Nat. Phys. ***10****, 845 (2014)*

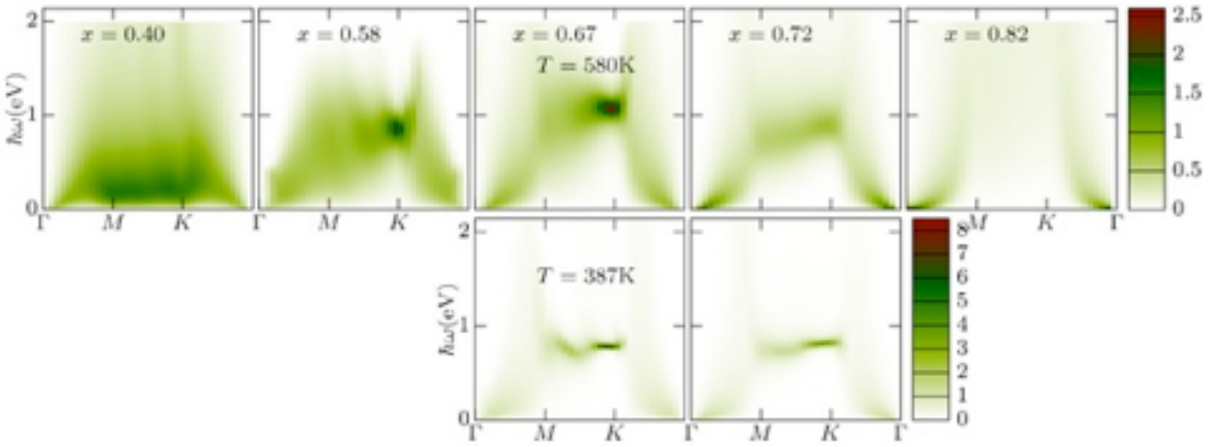

Na_xCoO_2
single-orbital, full DMFT treatment

L. Boehnke and F. Lechermann, pss ***221****, 1267 (2014)*

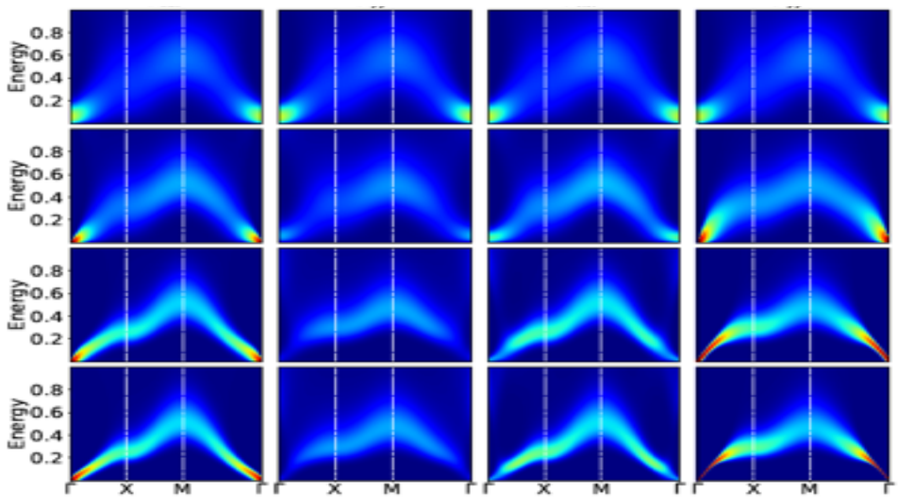

2-orbital Hubbard model, spontaneous
symmetry breaking, full DMFT treatment

D. Geffroy et al. PRL ***122****, 127601 (2019)*

LDA+DMFT approach to RIXS in correlated materials

Hybridization function V(ε)

$$V_\gamma^2(\varepsilon) = \sum_i |\langle \psi_{\gamma,i}|\hat{V}_{\mathrm{imp-host}}|d_\gamma\rangle|^2 \delta(\varepsilon - \varepsilon_{\gamma,i})$$

$$= -\frac{1}{\pi}\,\mathrm{Im}\,\langle d_\gamma|\hat{V}_{\mathrm{imp-host}}\frac{1}{\varepsilon - H_{\mathrm{host}}(\varepsilon)}\hat{V}_{\mathrm{host-imp}}|d_\gamma\rangle$$

$\Delta(\varepsilon)$

$$\Delta(\varepsilon) = \varepsilon - H_{\mathrm{imp}} - \Sigma(\varepsilon) - G^{-1}(\varepsilon)$$

DMFT self-energy

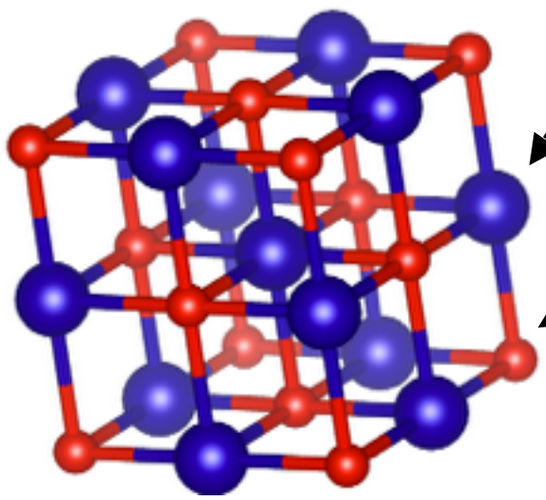

Ni (1/2, 1/2, 0)

O (1/2, 1/2, 1/2)

Hybridization function of Ni Eg orbital

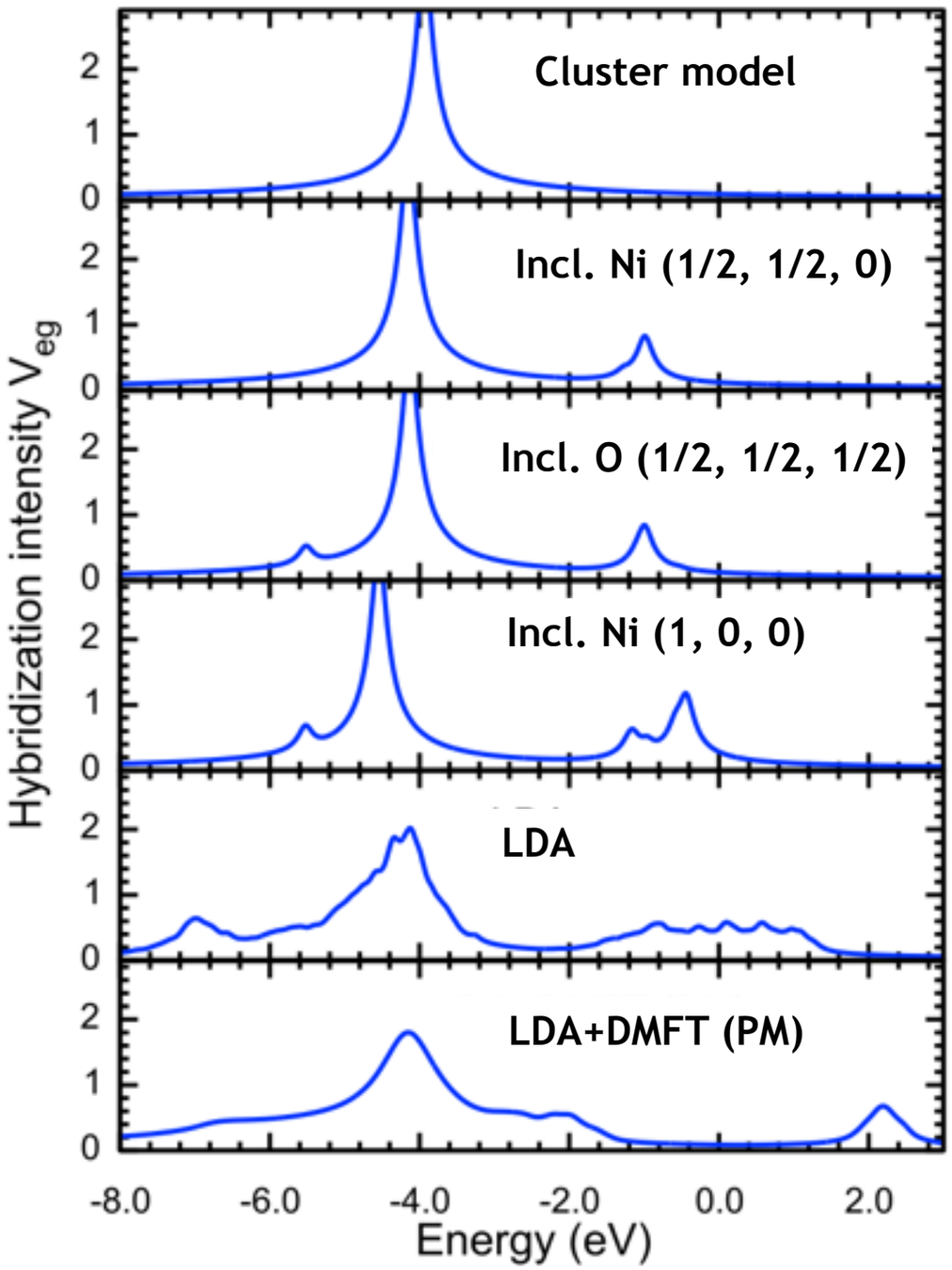

LDA+DMFT approach : Computational details

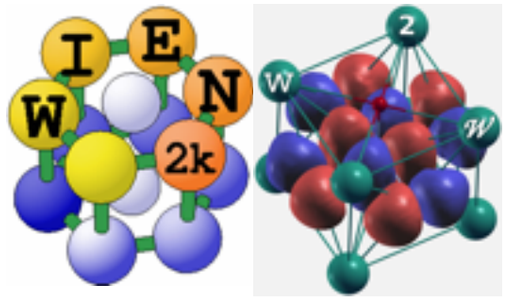

LDA+DMFT :

LDA, tight-binding model : Wien2K + Wien2wannier + Wannier90

DMFT self-consistency : Continuous-time quantum Monte Carlo solver

RIXS calculation : Configuration interaction method

Fine bath discretization (~25 levels per spin, orbital)

Efficient basis truncation (G.S theory + α)

3 (2) holes (electrons) below (above) Fermi energy

Lanczos diagonalization + Conjugate Gradient method

(with shift & seed switching)

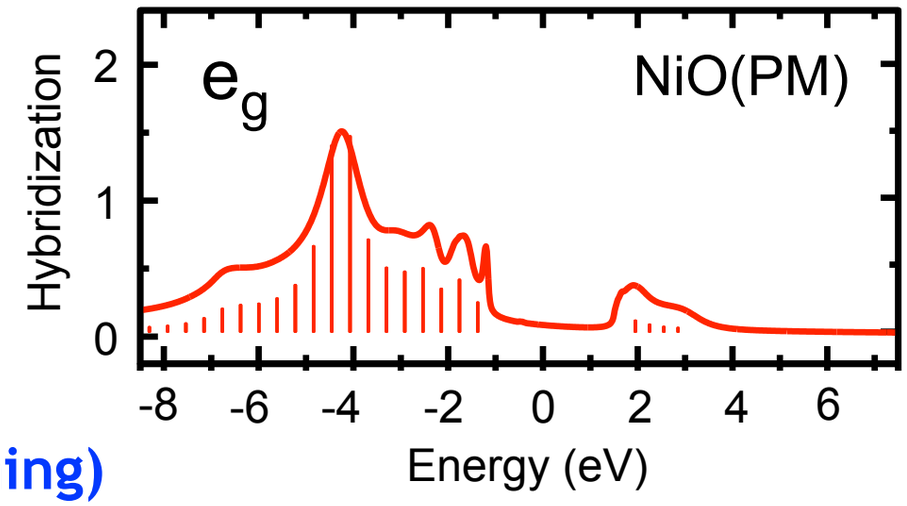

|g> : Lanczos method

$$F_{\mathrm{RIXS}}(\omega_{\mathrm{out}},\omega_{\mathrm{in}}) = \sum_f \left| \sum_m \frac{\langle f|T_{\mathrm{e}}|m\rangle\langle m|T_{\mathrm{i}}|g\rangle}{\omega_{\mathrm{in}} + E_g - E_m + i\Gamma_{\mathrm{L}}} \right|^2 \times \delta(\omega_{\mathrm{in}} + E_g - \omega_{\mathrm{out}} - E_f)$$

$$= \sum_f \left| \langle f|T_{\mathrm{e}} \frac{1}{\omega_{\mathrm{in}} + E_g - H_{\mathrm{imp}} + i\Gamma_{\mathrm{L}}} T_{\mathrm{i}}|g\rangle \right|^2 \times \delta(\omega_{\mathrm{in}} + E_g - \omega_{\mathrm{out}} - E_f)$$

Conjugated Gradient method (shift technique for ω_{in})

Benchmark : Ni L-edge RIXS in NiO

A unified description of core-level RIXS, XAS, XPS and valence spectra

Valence spectra

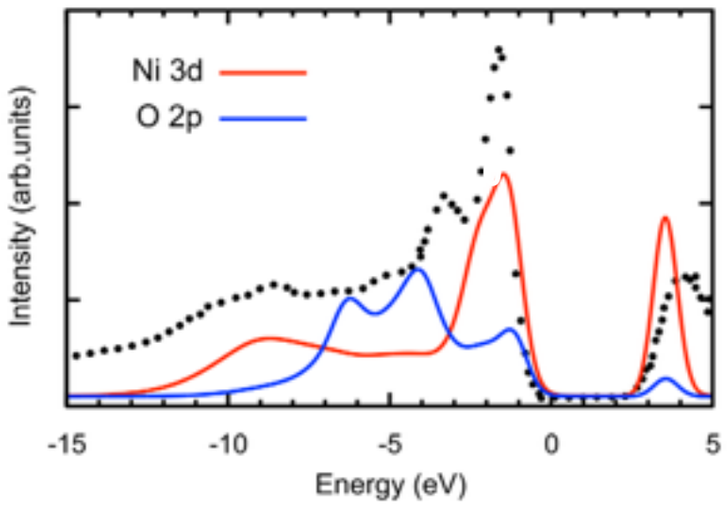

Ni L-edge XAS

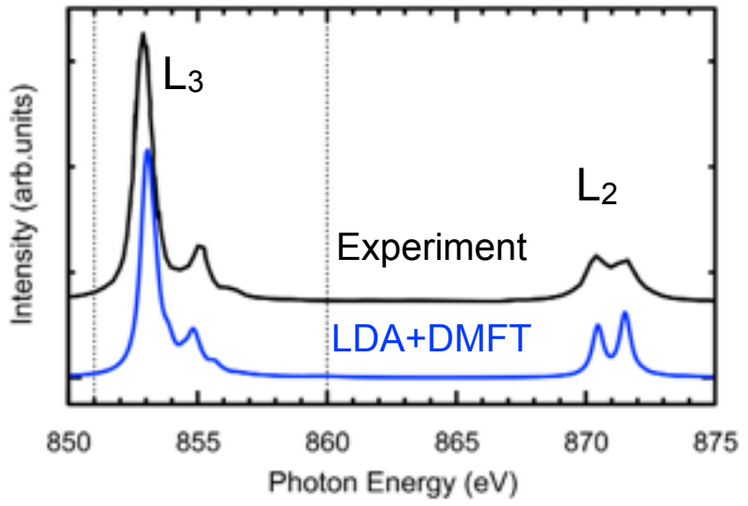

Ni L-edge RIXS

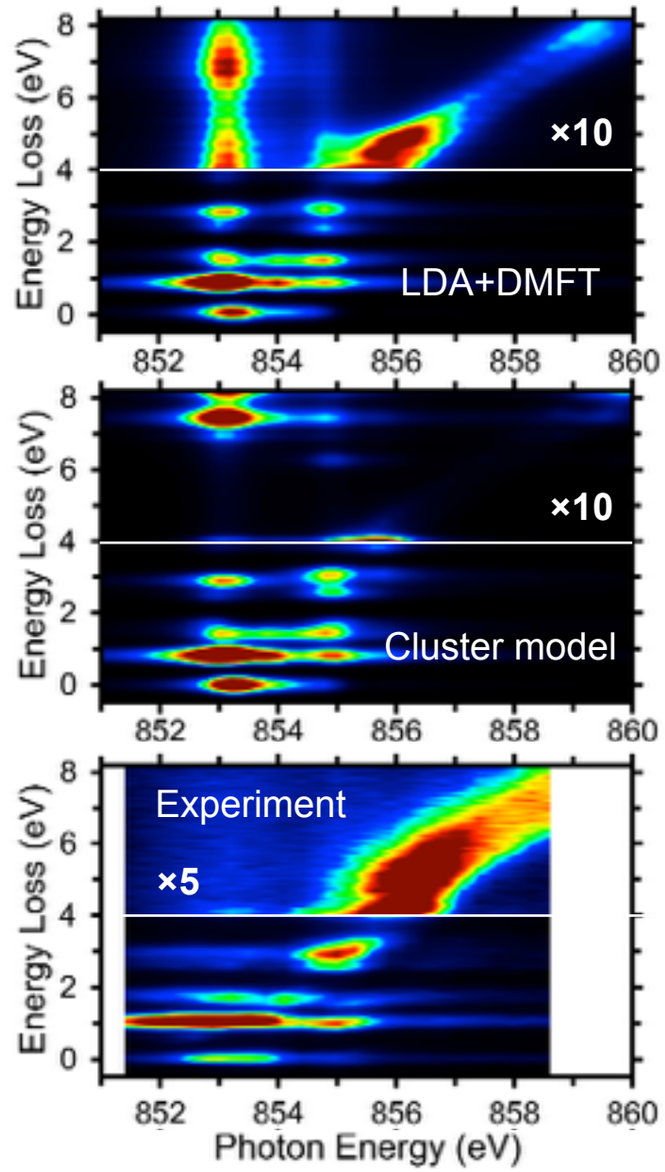

Hybridization function

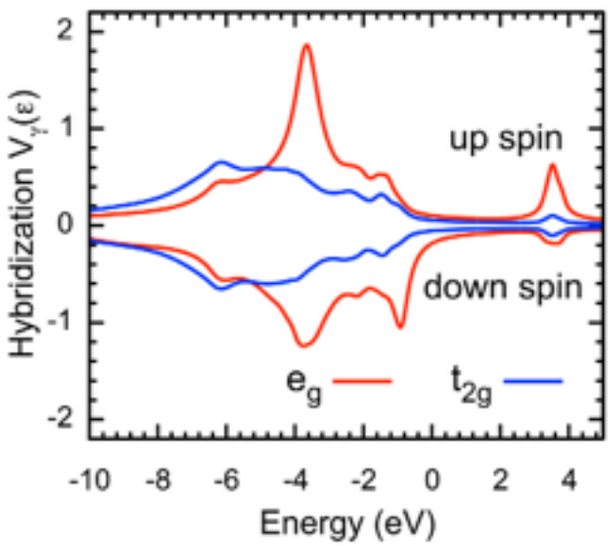

Ni L-edge XPS

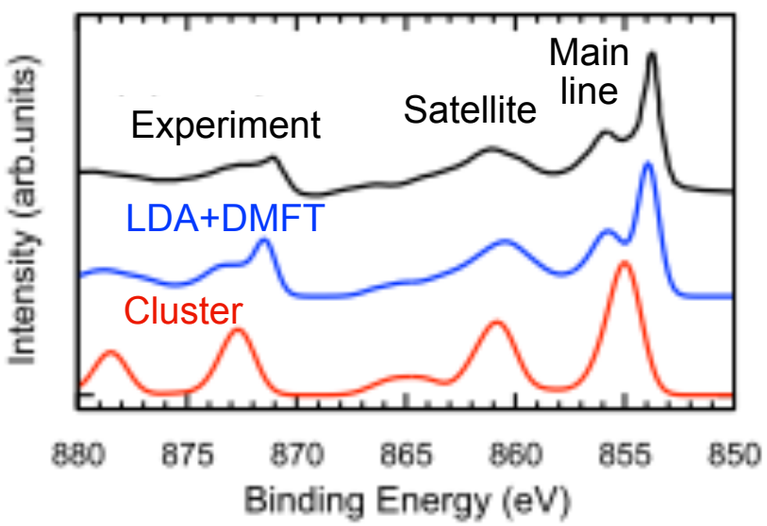

Good agreement with the experimental RIXS data

- dd excitations (0~4eV) : multiplet, crystal field
- CT excitations (4~8eV) : local and nonlocal CT
- unbound excitations (4eV~) : fluorescence-like feature

Experimental data

Valence XPS : G. A. Sawatzky et al. PRL **53**, 2339 (1984)
L-edge XAS : D. Alders et al. PRB **57**, 11623 (1998)
L-edge XPS : M. Taguchi et al. PRL **100**, 206401 (2008)
L-edge RIXS : G. Ghiringhelli et al. PRL **102**, 027401 (2009)

Benchmark : Fe L-edge RIXS in Fe_2O_3

A unified description of core-level RIXS, XAS, XPS and valence spectra

Valence spectra

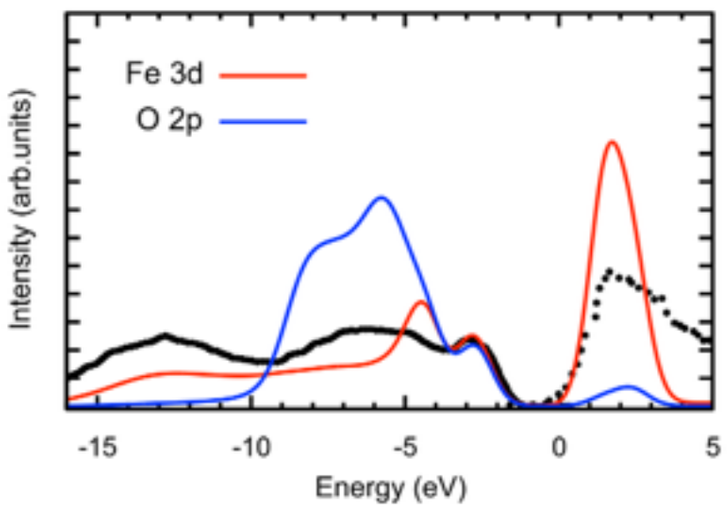

Fe L-edge XAS

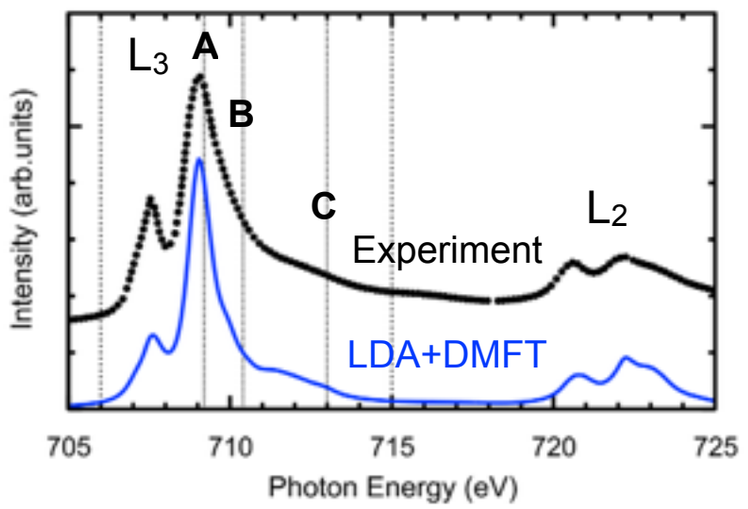

Fe L-edge RIXS

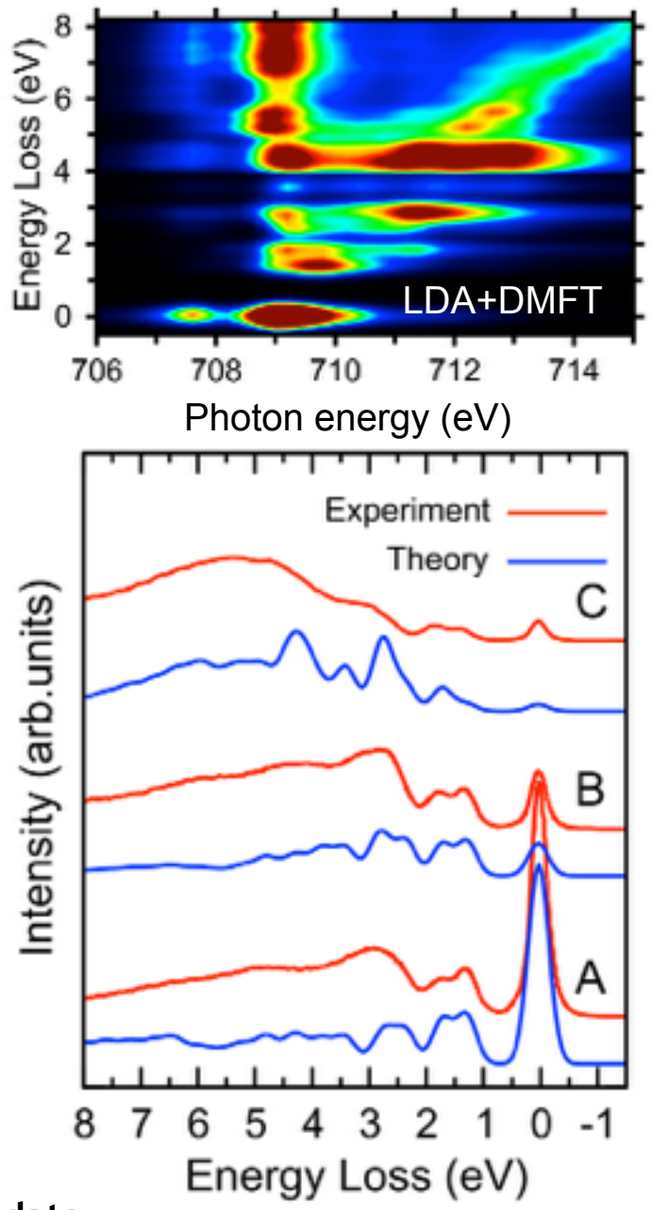

Hybridization function

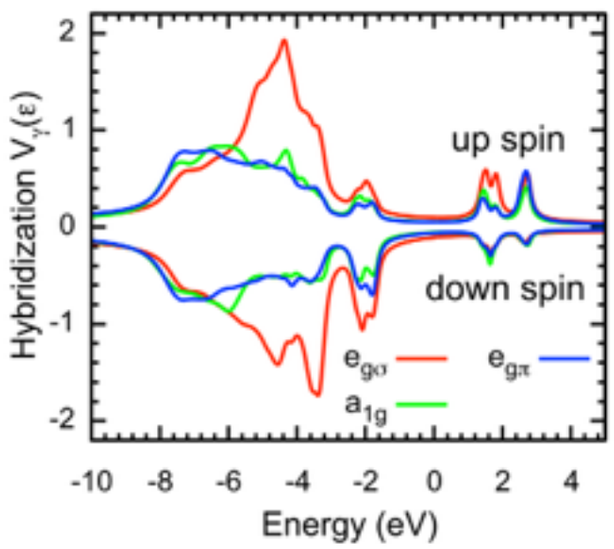

Fe L-edge XPS

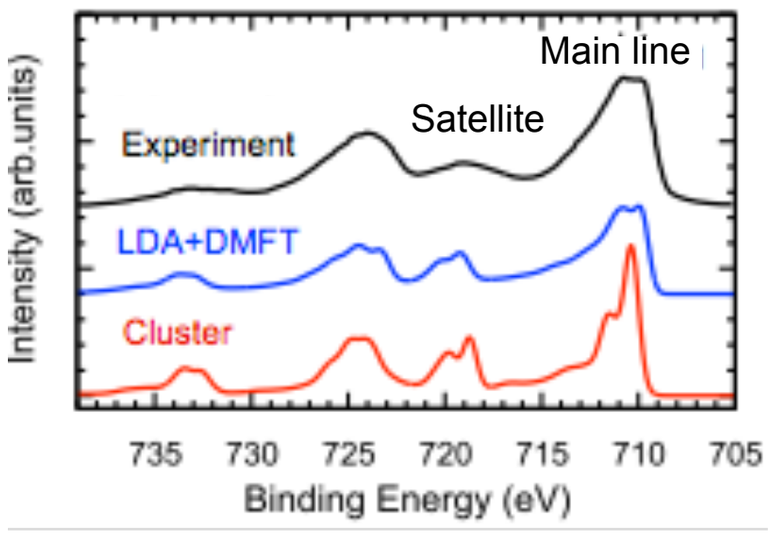

Good agreement with the experimental RIXS data

- dd excitations (0~4eV) : multiplet, crystal field
- CT excitations (4~8eV) : local and nonlocal CT
- unbound excitations (4eV~) : fluorescence-like feature

Experimental data

Valence PES/BIS : F. Ciccacci et al. PRB **44**, 10444 (1991)
R. J. Lad et al. PRB **39**, 13478 (1898

L-edge XAS : M. L. Yang et al. PRB **80**, 014508 (2017)

L-edge XPS : M. Miedema et al. JESRP **203**, 8 (2015)

L-edge RIXS : J. Miyawaki et al. 96, 214420 (2017)

RIXS and XAS in high-valence transition-metal oxides

Received 13 Mar 2016 | Accepted 25 Aug 2016 | Published 11 Oct 2016

DOI: 10.1038/ncomms13017 OPEN

Ground-state oxygen holes and the metal–insulator transition in the negative charge-transfer rare-earth nickelates

Valentina Bisogni[1,2], Sara Catalano[3], Robert J. Green[4,5], Marta Gibert[3], Raoul Scherwitzl[3], Yaobo Huang[1,6], Vladimir N. Strocov[1], Pavlo Zubko[3,7], Shadi Balandeh[4], Jean-Marc Triscone[3], George Sawatzky[4,5] & Thorsten Schmitt[1]

$NdNiO_3$

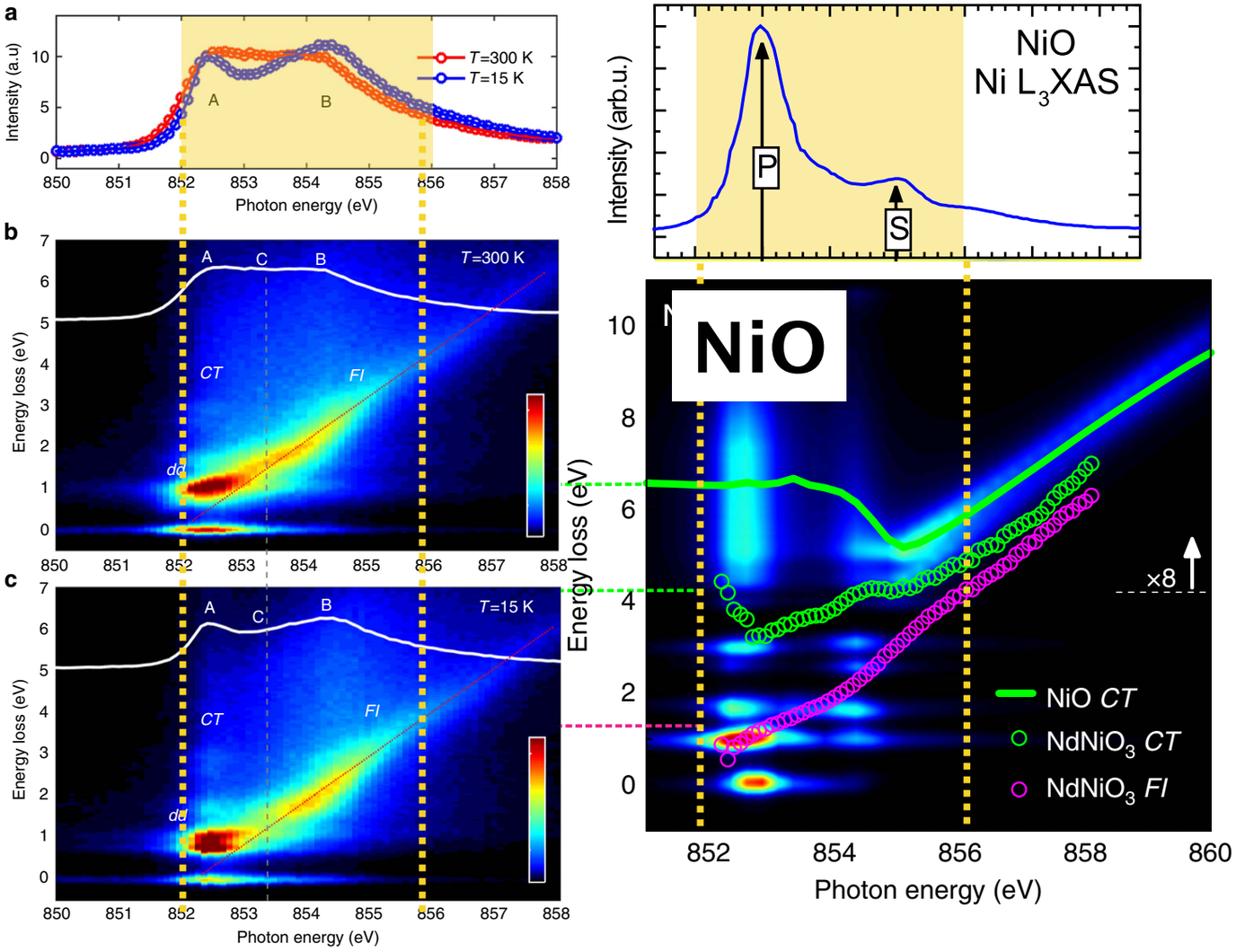

Double-cluster studies

R. J. Green et al. PRB **94**, 195127

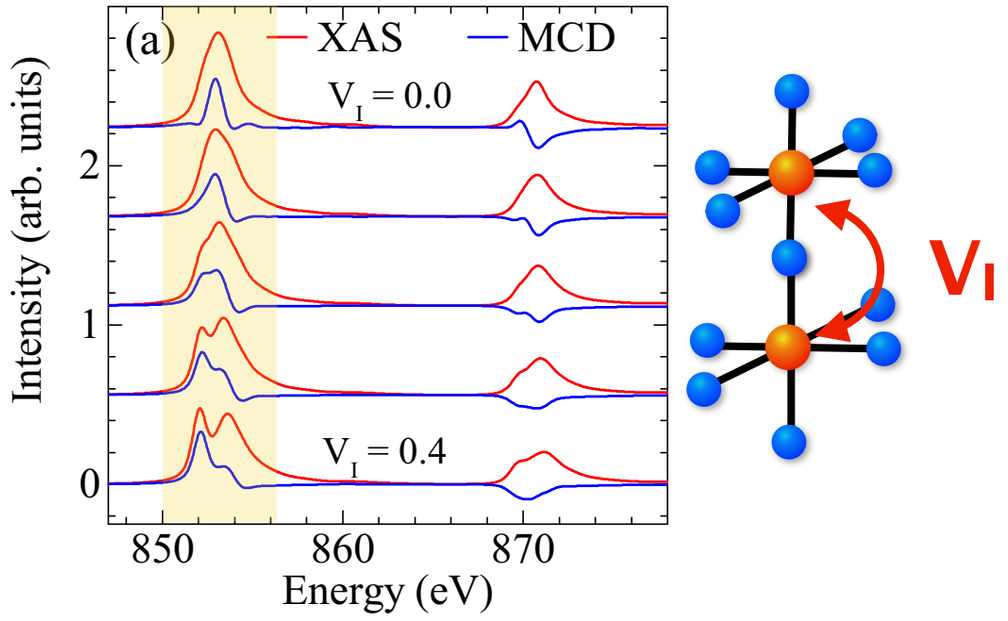

Y. Lu et al. PRX **8**, 031014

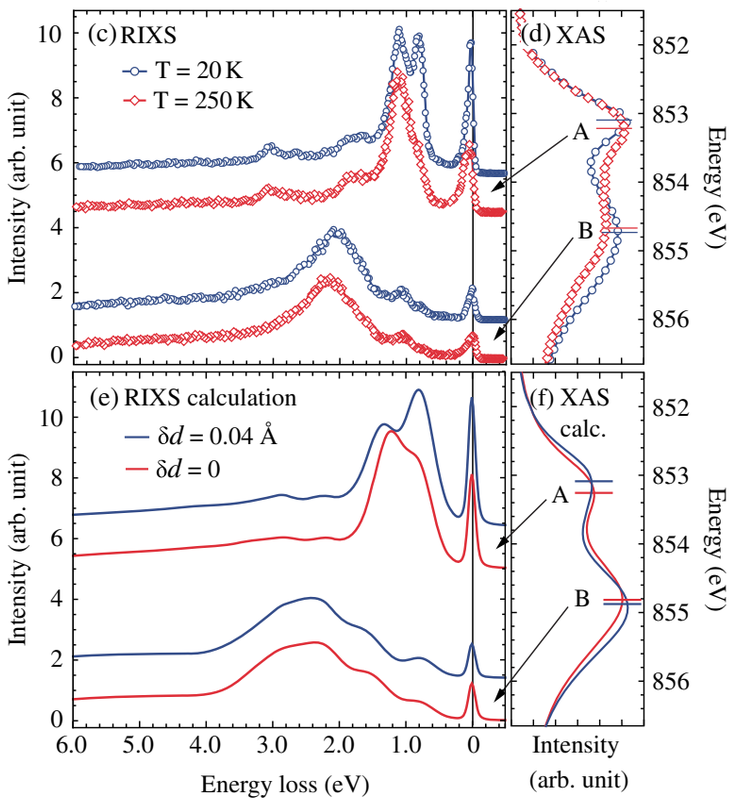

Ni L_3-RIXS in $LuNiO_3$: LDA+DMFT

Paramagnetic insulating phase
($T_{lattice}$=533K < T_{MI})

Valence spectra

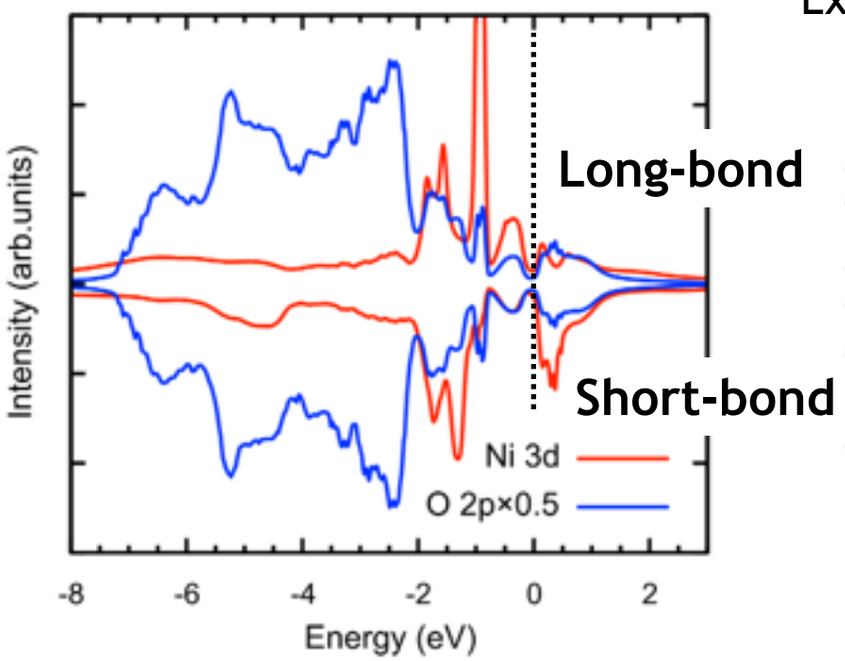

Ni L-edge XAS)*

Exp. C. Piamonteze et al PRB **71**, 020406 (2005)

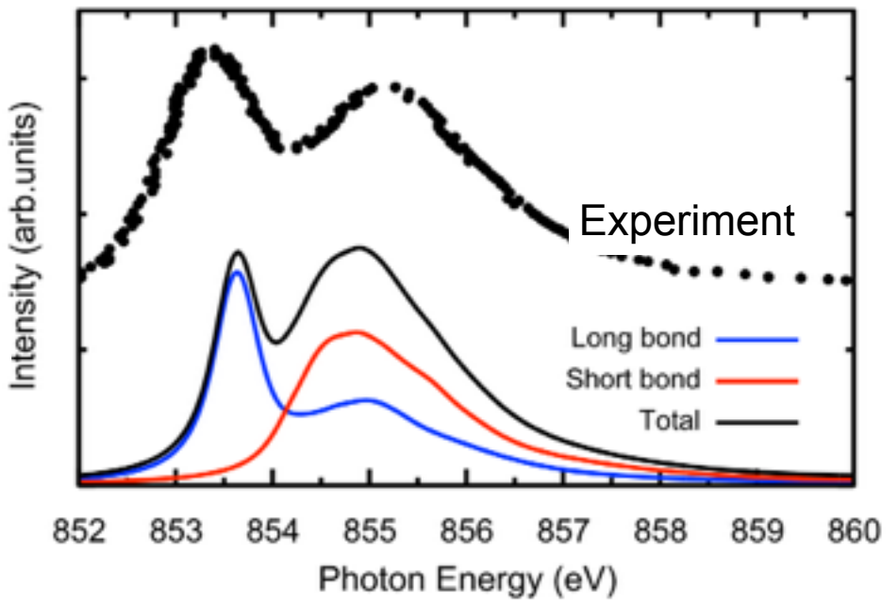

Ni L-edge RIXS

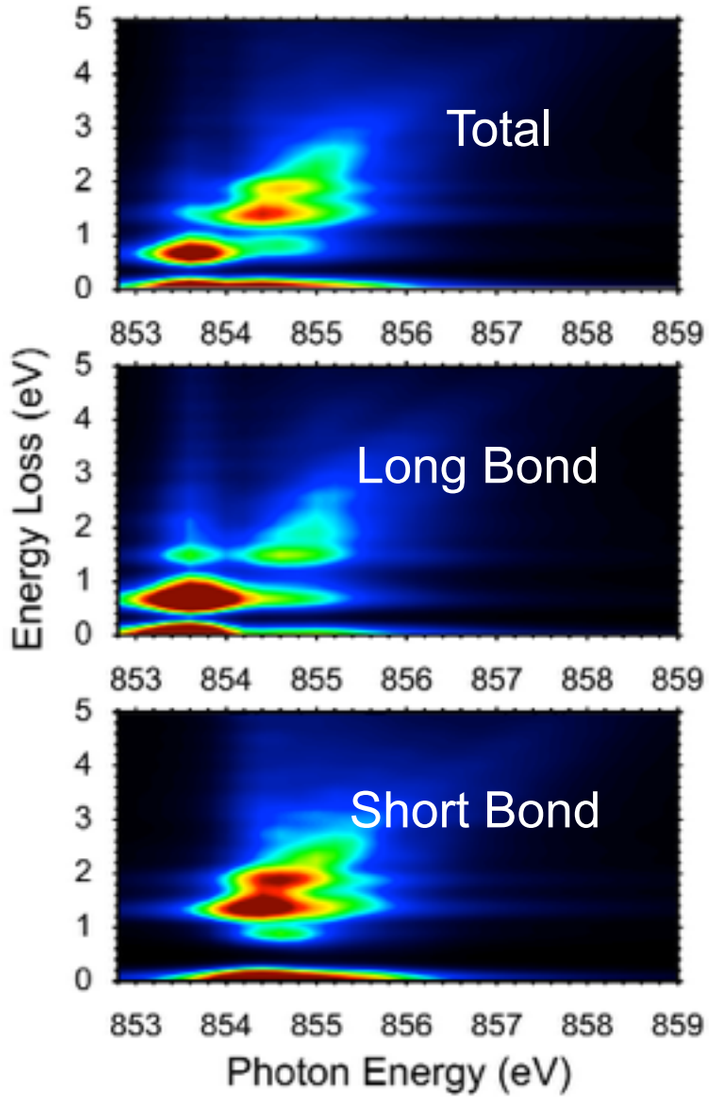

Hybridization function

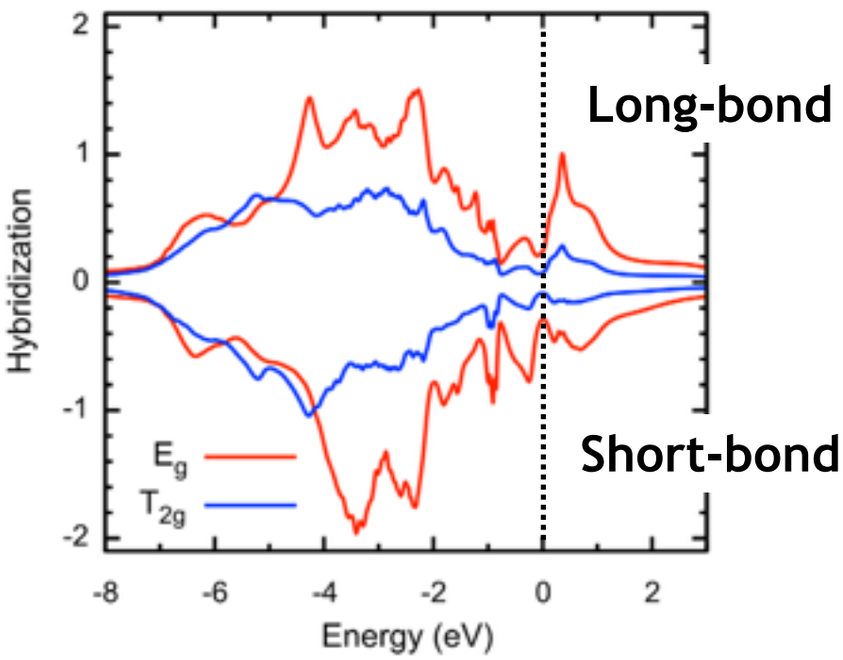

long-bond NiO_6

Short-bond
NiO_6

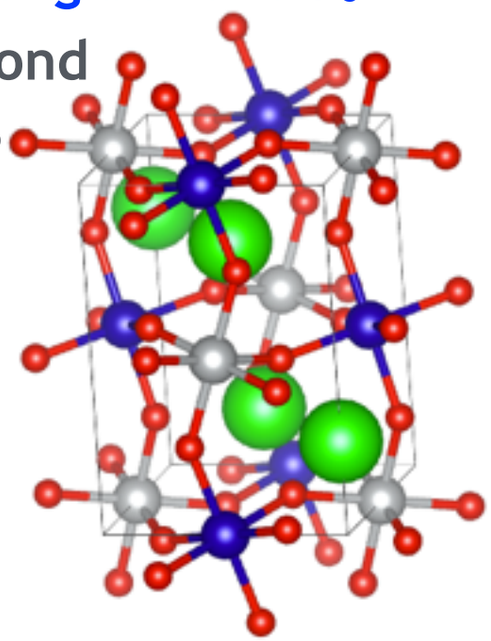

)* core-level shift (LDA) ~0.4eV
(not included in these results)

Cu L_3-RIXS in $LaCuO_3$ and $NaCuO_2$

Two isoelectronic high-valence cuprates (Cu^{3+})

$LaCuO_3$ $NaCuO_2$

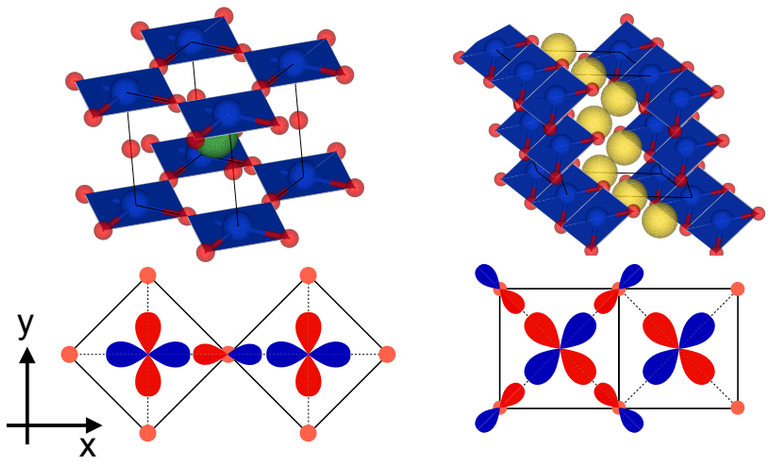

$RNiO_3$ V. Bisogni et al. (2016)

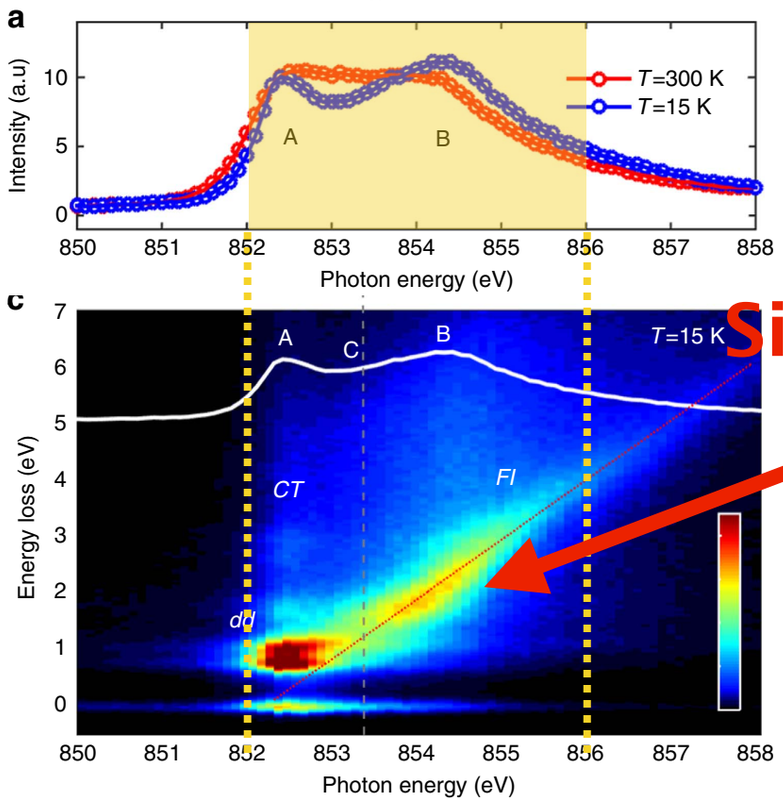

Calc. Cu L-edge XAS and RIXS (LDA+DMFT)

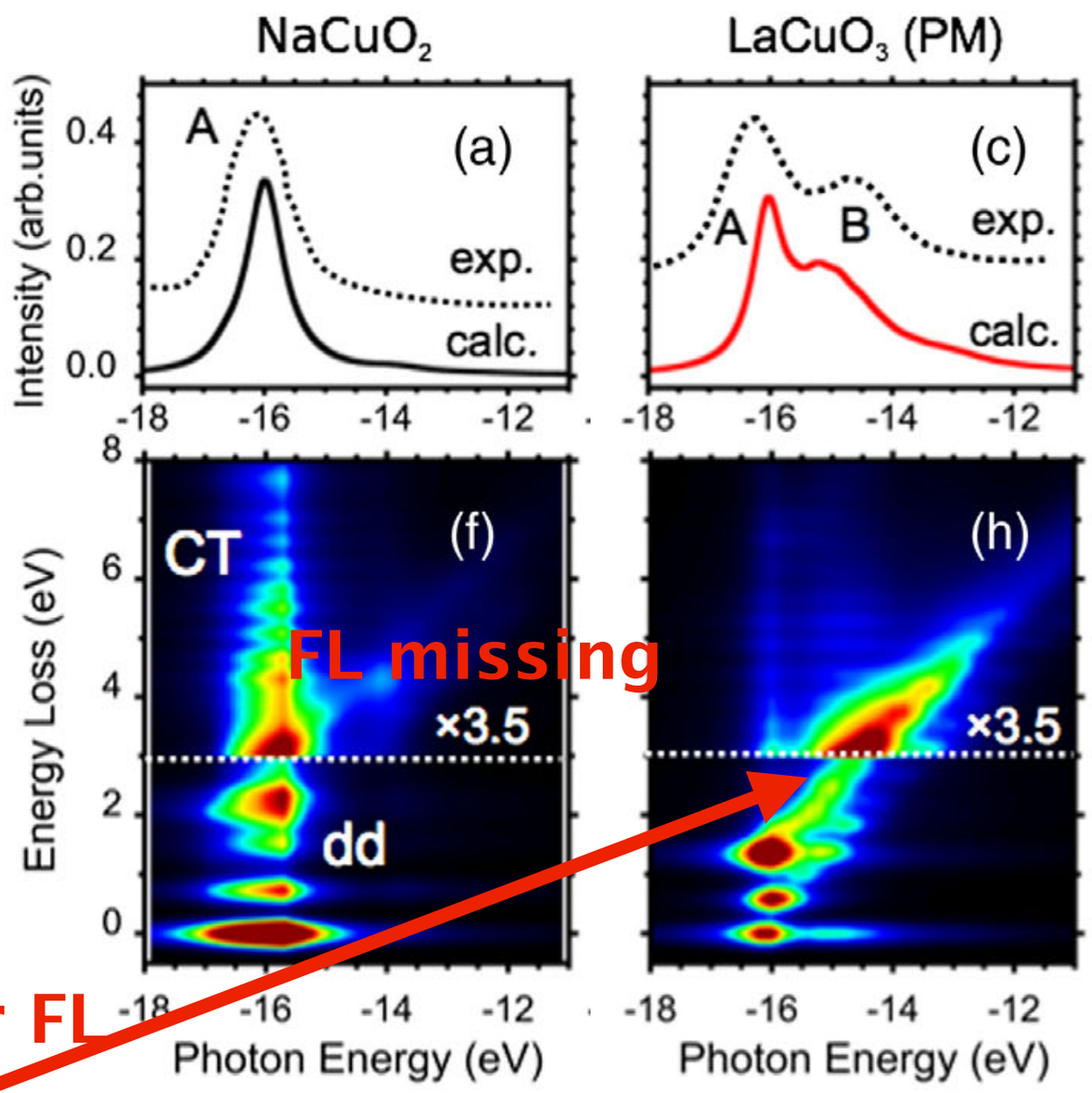

Similar FL

A. Hariki, M. Winder, and JK, PRL **121**, 126403 (2018)

What determines the excitation rule of the unbound electron-hole continuum ?

Cu L_3-RIXS in $LaCuO_3$ and $NaCuO_2$

1P Valence spectra

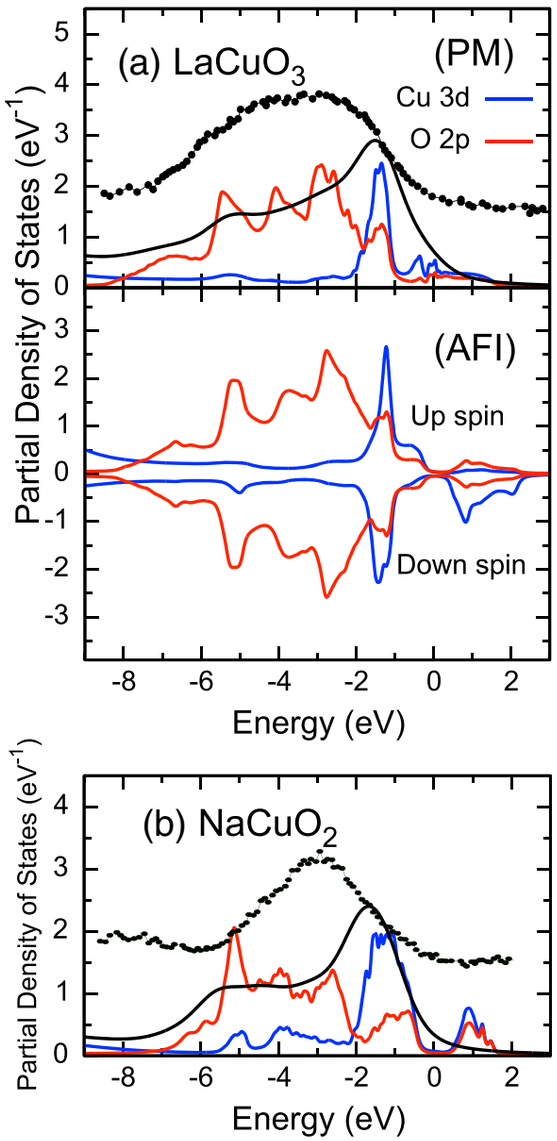

Hybridization V(ε)

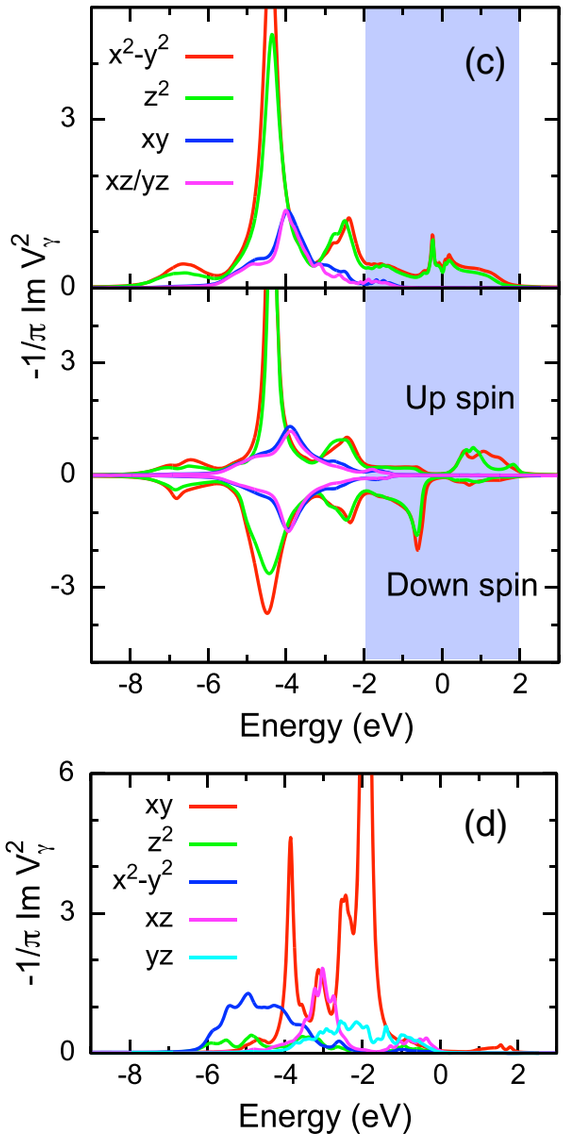

Calc. Cu L-edge XAS and RIXS (LDA+DMFT)

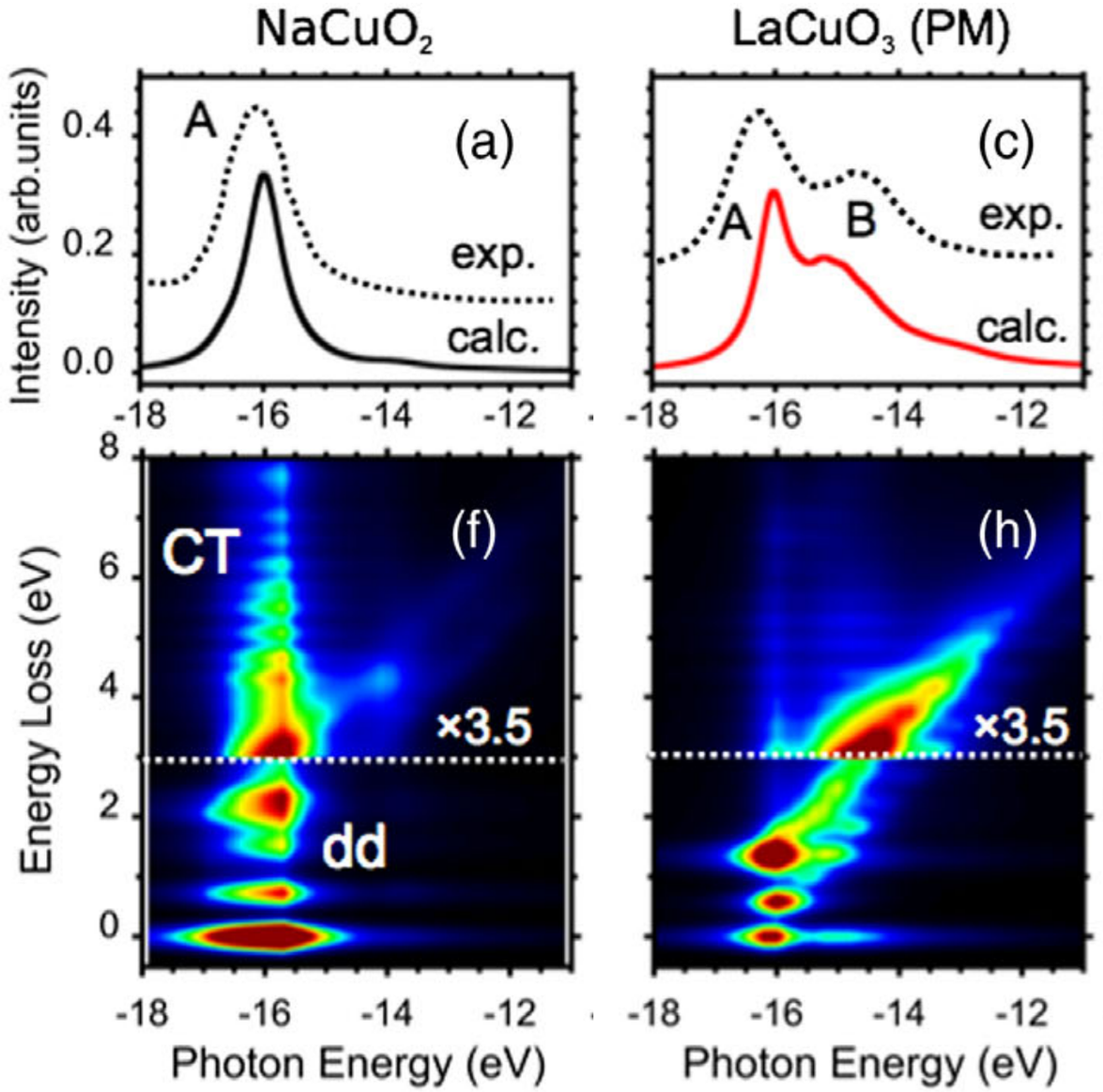

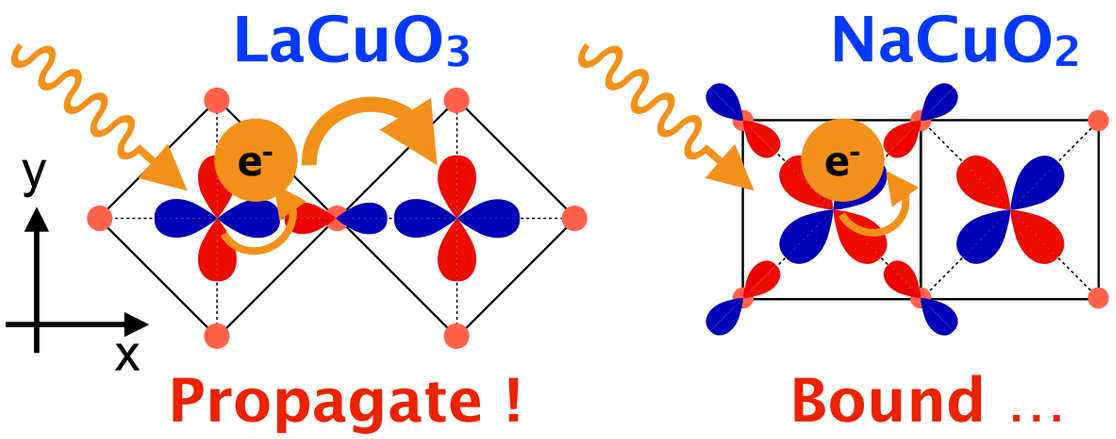

Hybridization function encodes excitation amplitude of electron-hole pair under material-specific lattice geometry !

q-dependent 2P excitations

Excitation spectrum in correlated materials

Excitonic physics in $LaCoO_3$ (Co^{3+}: d^6)

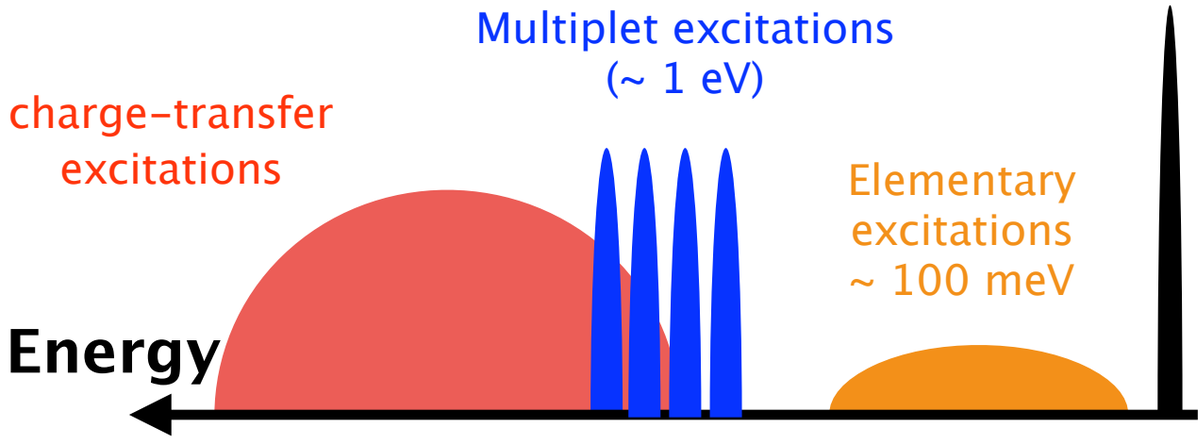

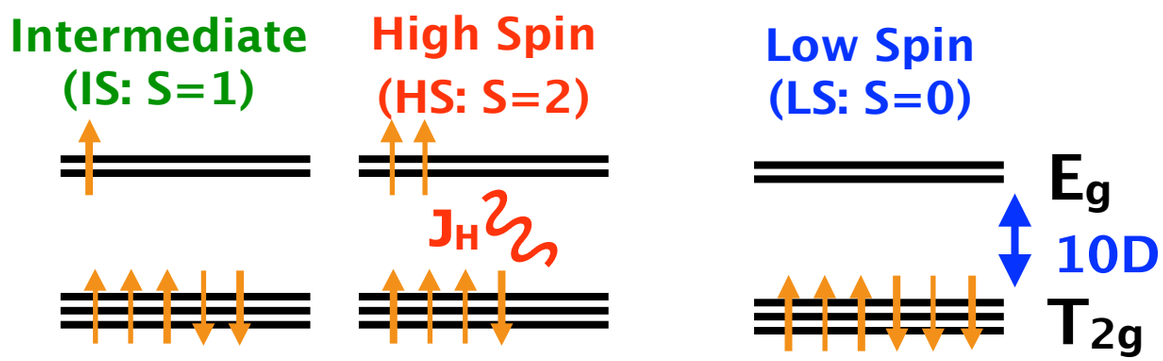

q-dependent 2P excitations

Excitation spectrum in correlated materials

Excitonic physics in $LaCoO_3$ (Co^{3+}: d^6)

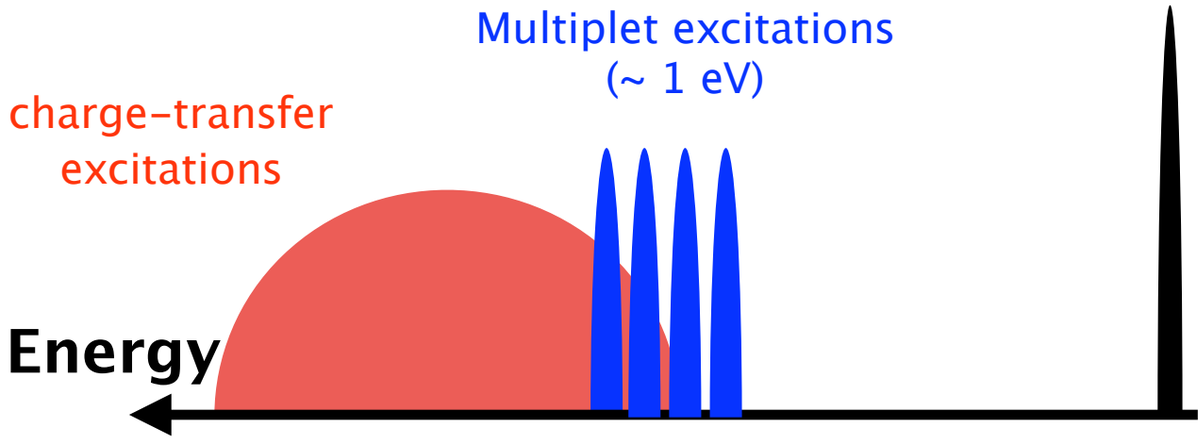

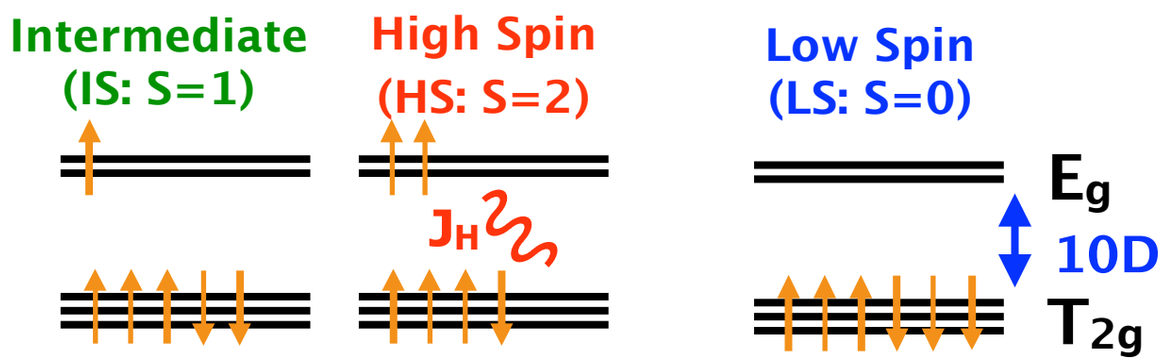

q-dependent 2P excitations

Excitation spectrum in correlated materials

Excitonic physics in $LaCoO_3$ (Co^{3+}: d^6)

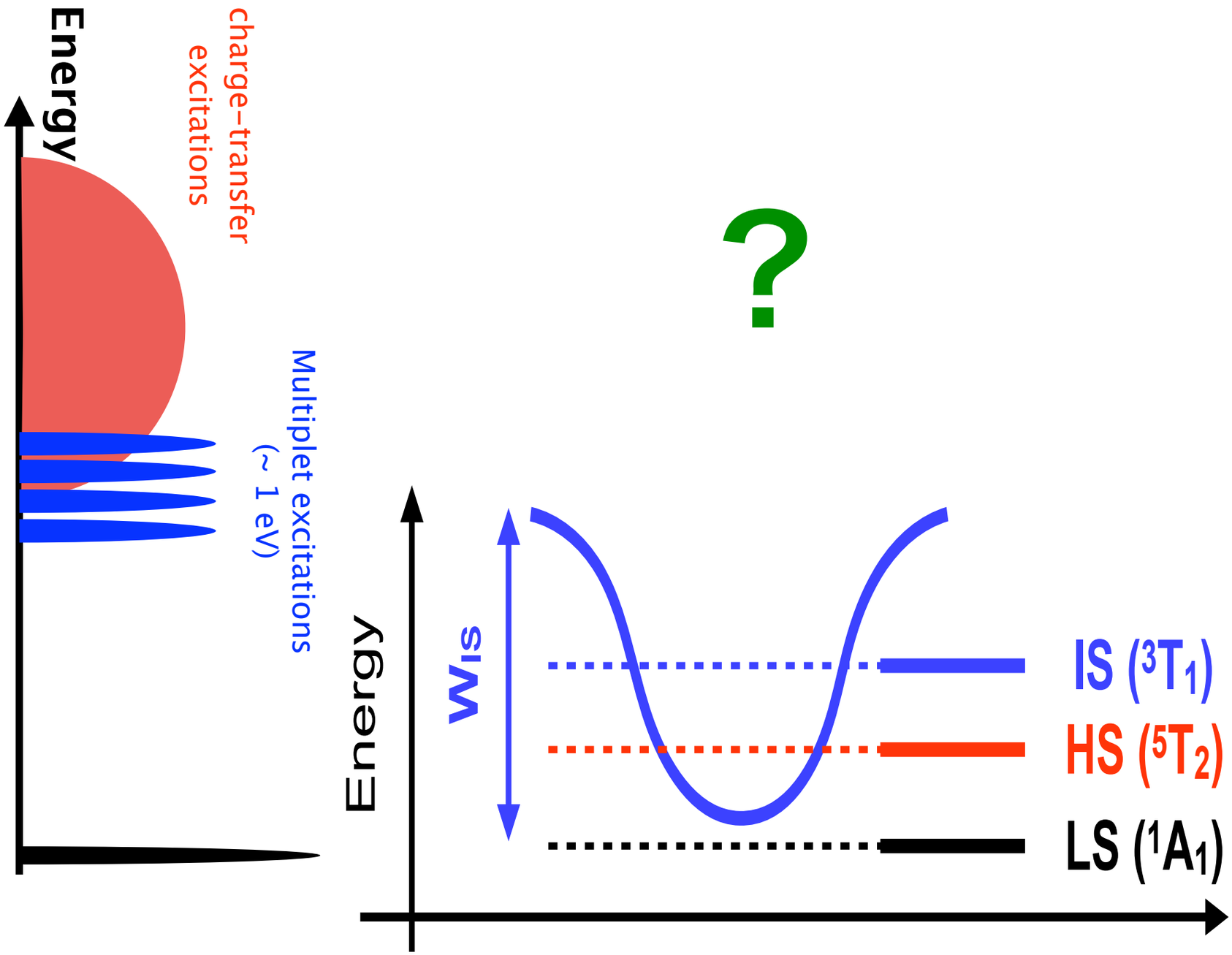

A. Sotnikov and JK, Sci. Rep. **6**, 30510 (2016)

q-dependent 2P excitations

Excitation spectrum in correlated materials

Excitonic physics in $LaCoO_3$ (Co^{3+}: d^6)

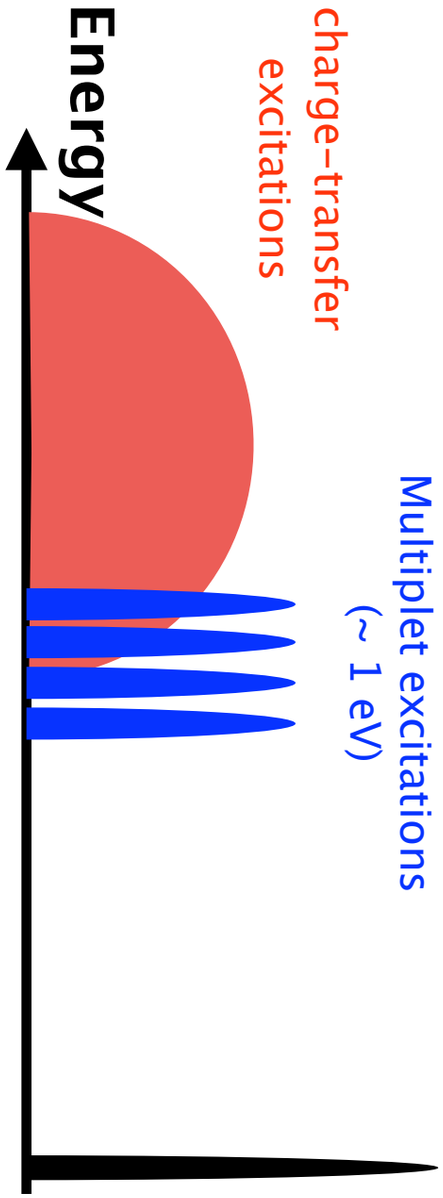

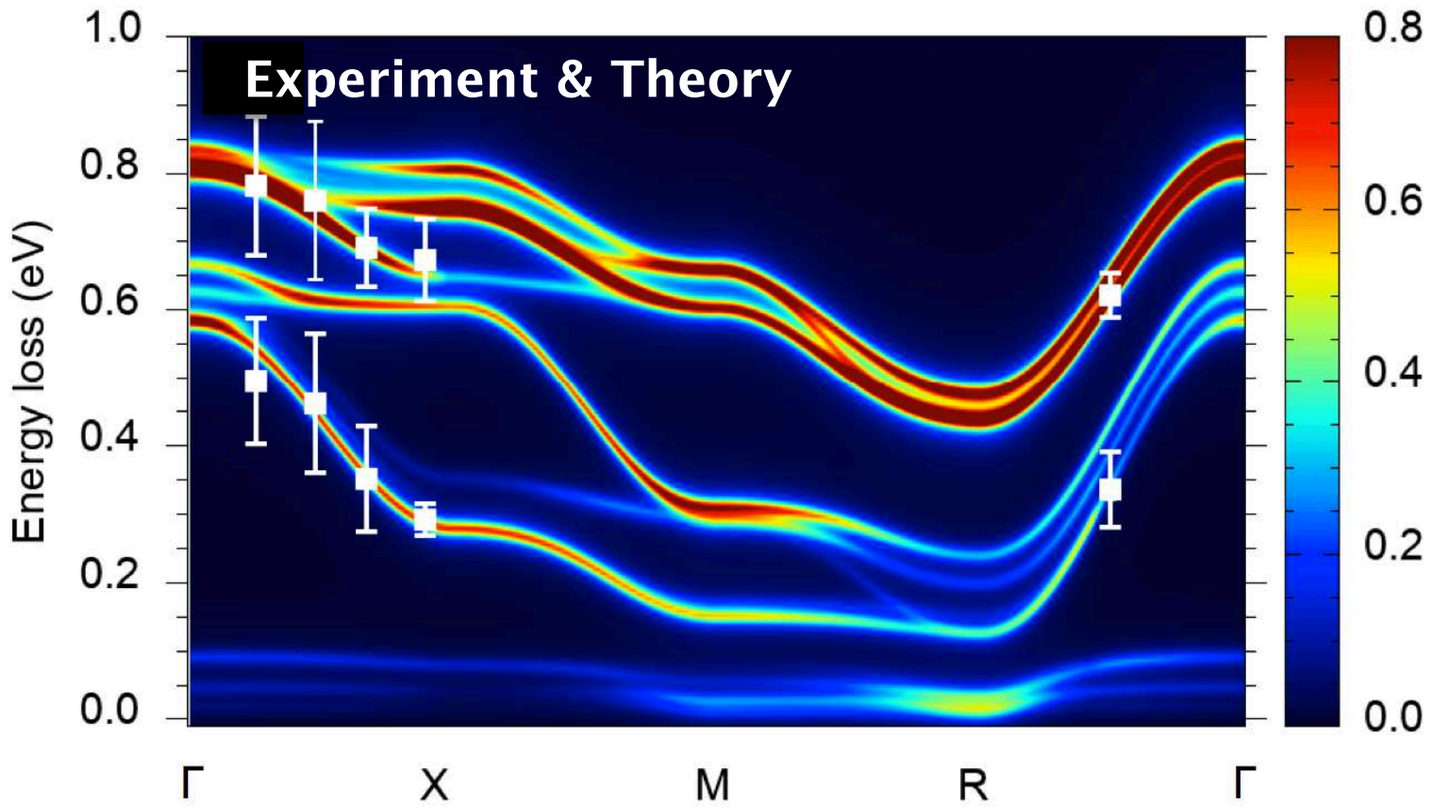

R.-P. Wang et al., PRB **98**, 035149 (2018)

Conclusion and future perspective

We developed computational method based on LDA+DMFT for calculation of core-level RIXS, XPS, XAS spectra in correlated materials

Anderson impurity model description with DMFT hybridization in RIXS analysis for correlated materials

Advantages :

1. description of both bound (dd) excitation and unbound electron-hole pairs
2. low computational cost, applicable to wide range of correlated materials including covalent or high-valance materials

Future:

k-dependence in RIXS spectra (within DMFT or + beyond)

Conclusion and fu

Comments on 2P function within DMFT ?

Future challenge :

Recover k-dependence in RIXS spectra (within DMFT or + beyond)

2-band Hubbard model near excitonic-condensation instability

1P spectra

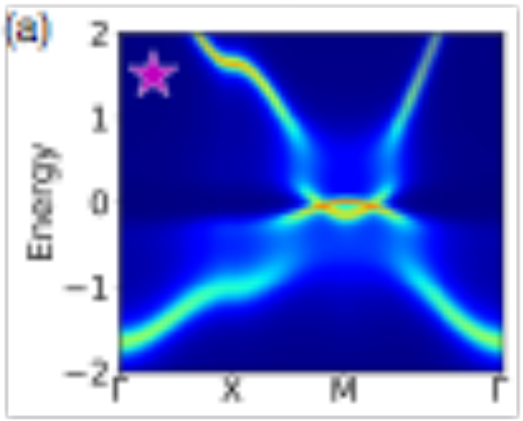

Phase diagram

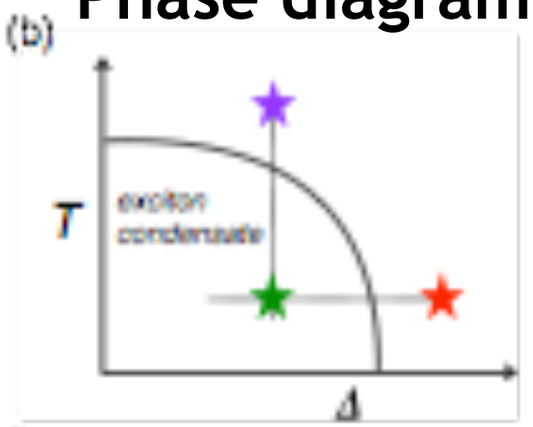

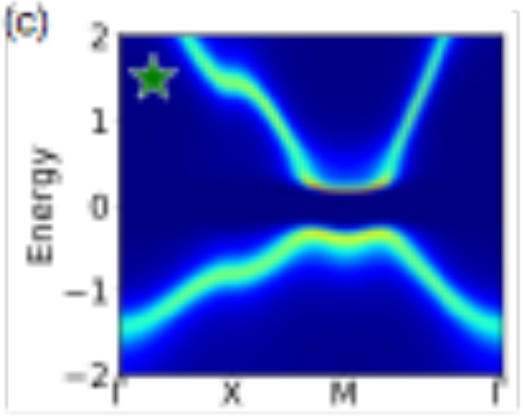

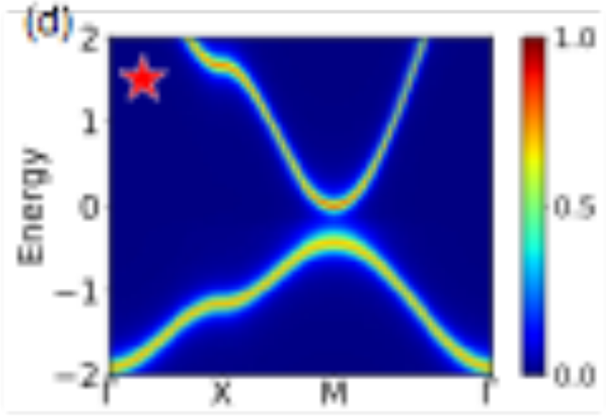

D. Geffroy et al. PRL 122, 127601 (2019)

2P spectra (dynamical susceptibility)

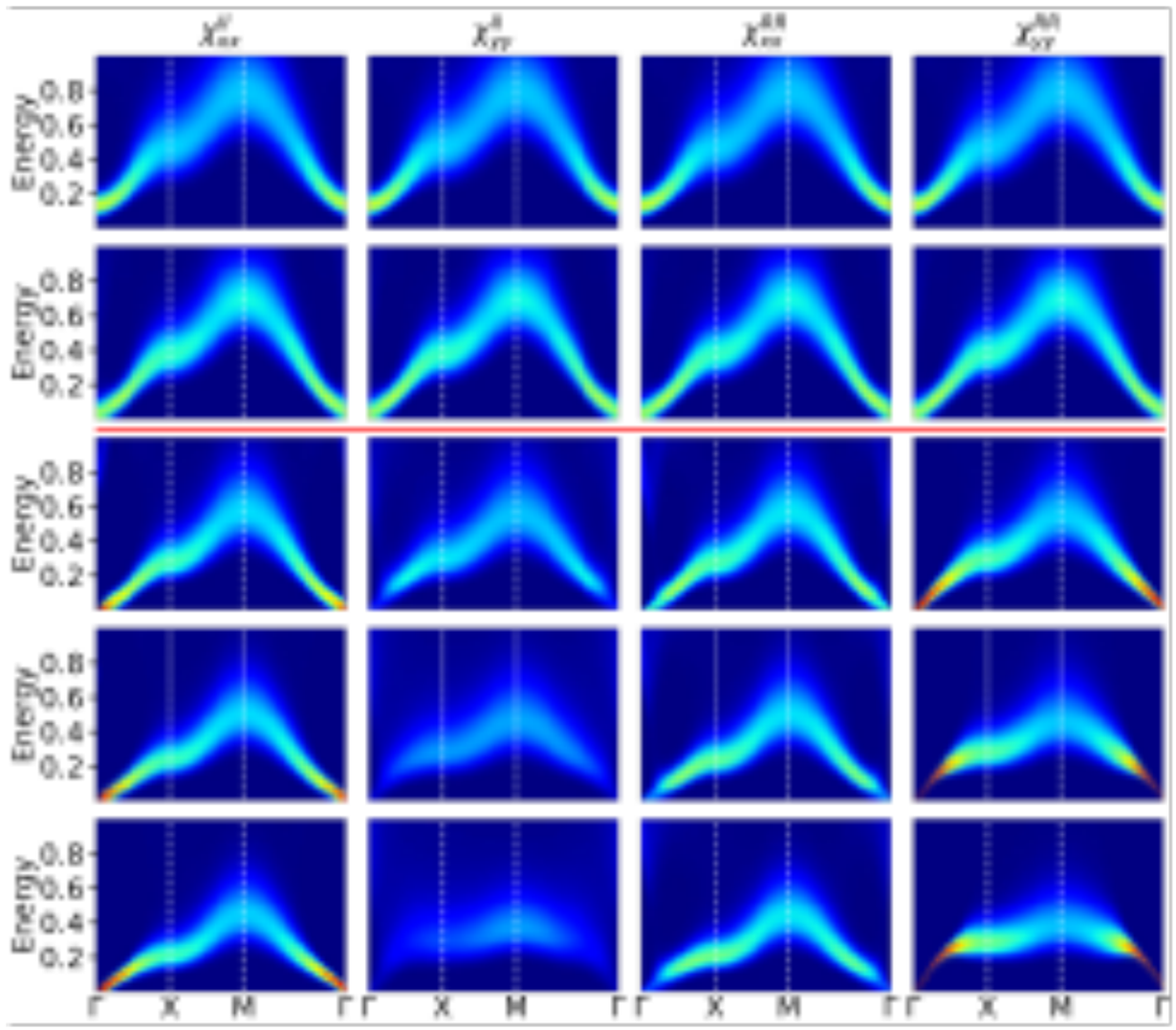

$$\chi^{OO}_{\eta\eta'}(\mathbf{k}, i\nu_n) = \sum_{\mathbf{R}} \int_0^\beta d\tau e^{i(\nu_n \tau + \mathbf{k}\cdot\mathbf{R})} \langle O^\eta_{\mathbf{i}+\mathbf{R}}(\tau) O^{\eta'}_{\mathbf{i}}(0) \rangle - \langle O^\eta \rangle^2$$

Benchmark : Ni L-edge RIXS in NiO

ALL data

Valence spectra

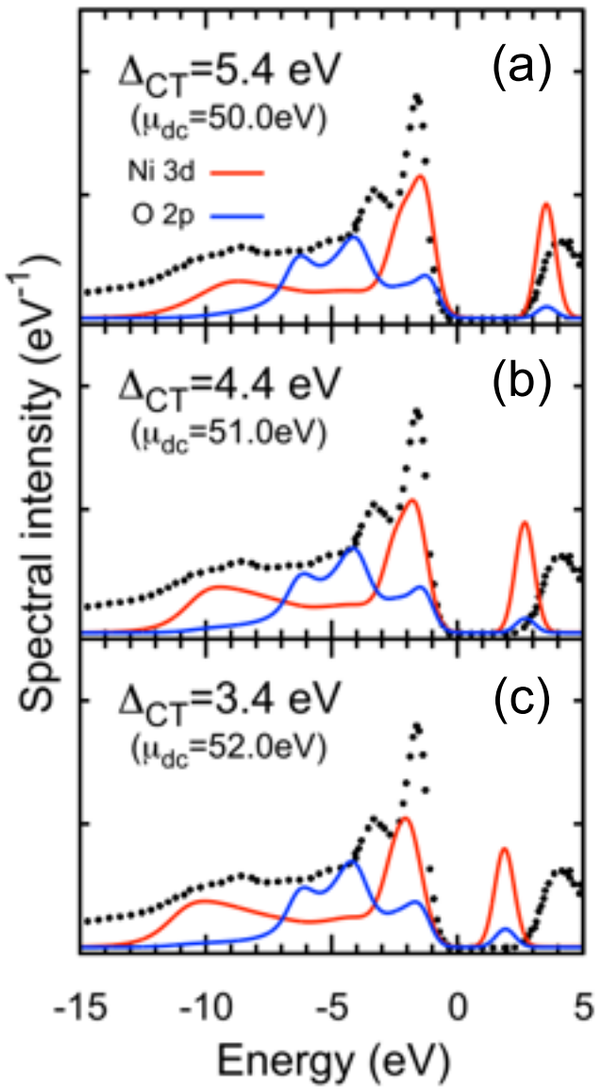

Ni L-edge XAS

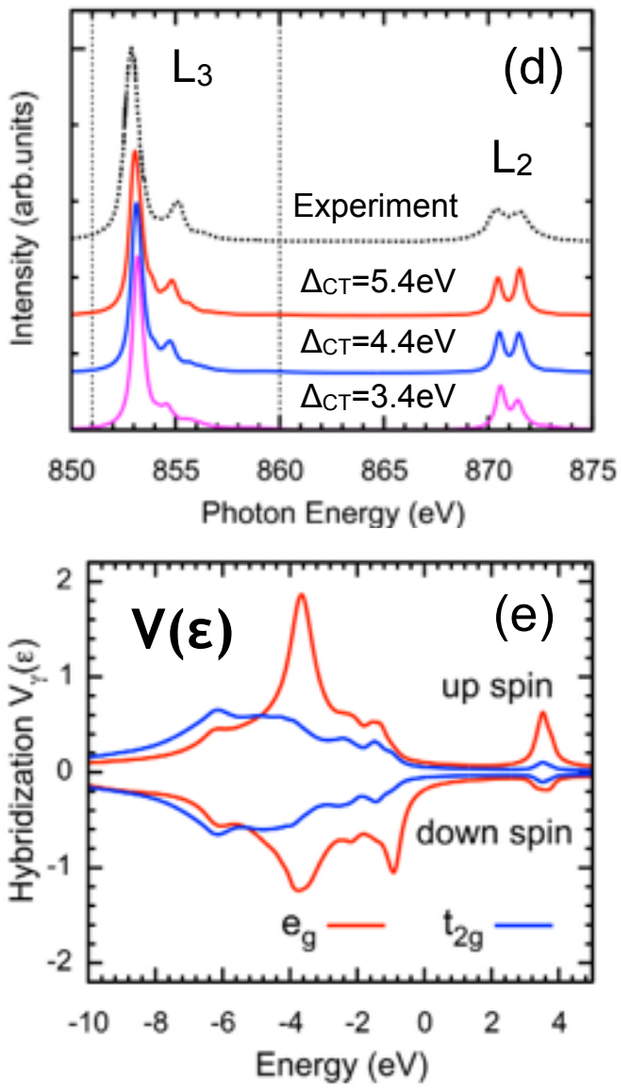

Ni L-edge RIXS

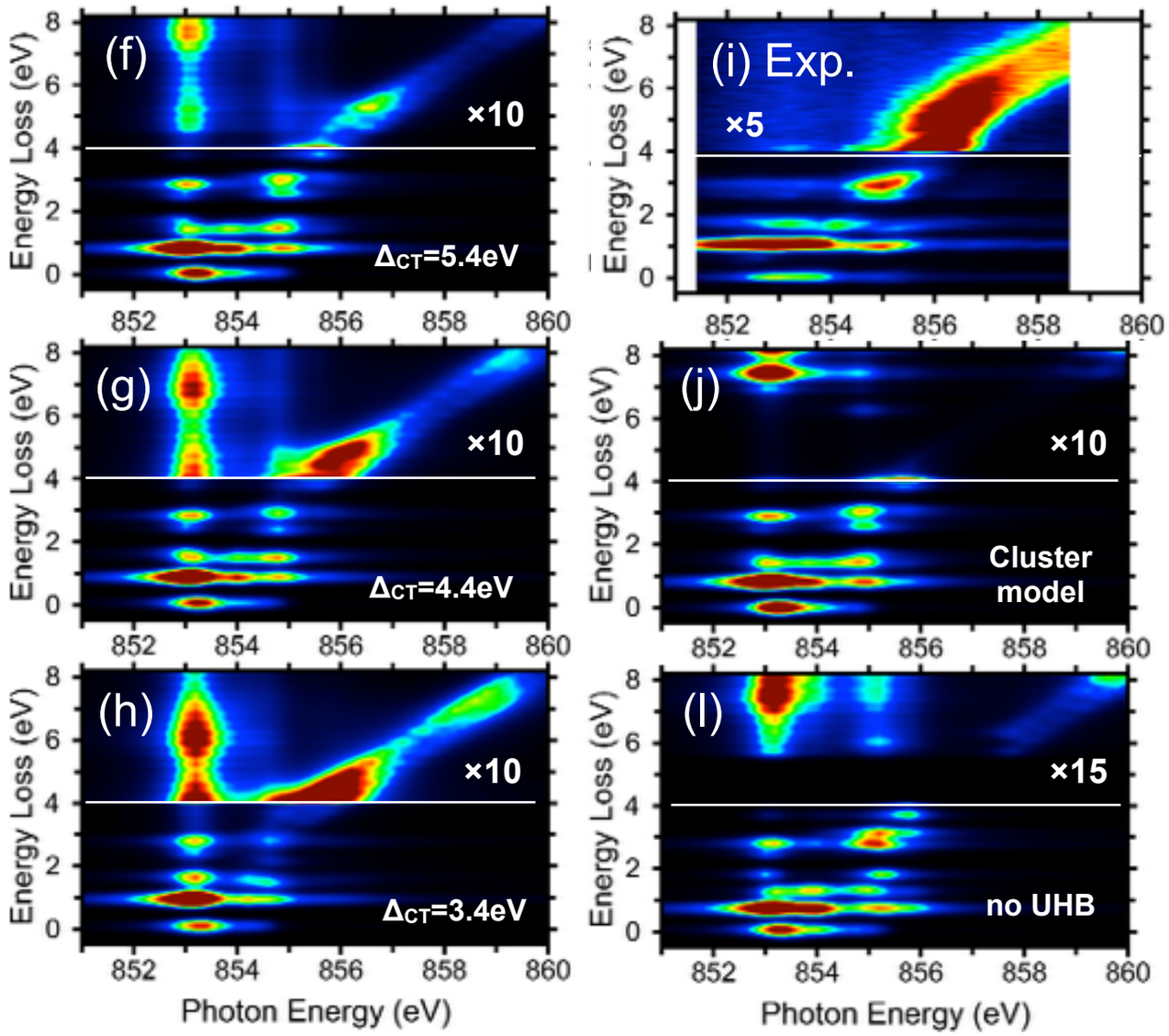

Good agreement with the experimental data

- **localized excitations (0~4eV) : multiplet, crystal field**
- **CT excitations (4-8eV) : local and nonlocal CT**
- **unbound excitations (4eV~: fluorescence-like feature)**

Experimental data

valence XPS : G. A. Sawatzky et al. PRL **53**, 2339 (1984)

L-edge XAS : D. Alders et al. PRB **57**, 11623 (1998)

L-edge RIXS : G. Ghiringhelli et al. PRL **102**, 027401 (2009)

Benchmark : Fe L-edge RIXS in Fe_2O_3

ALL data

Valence spectra

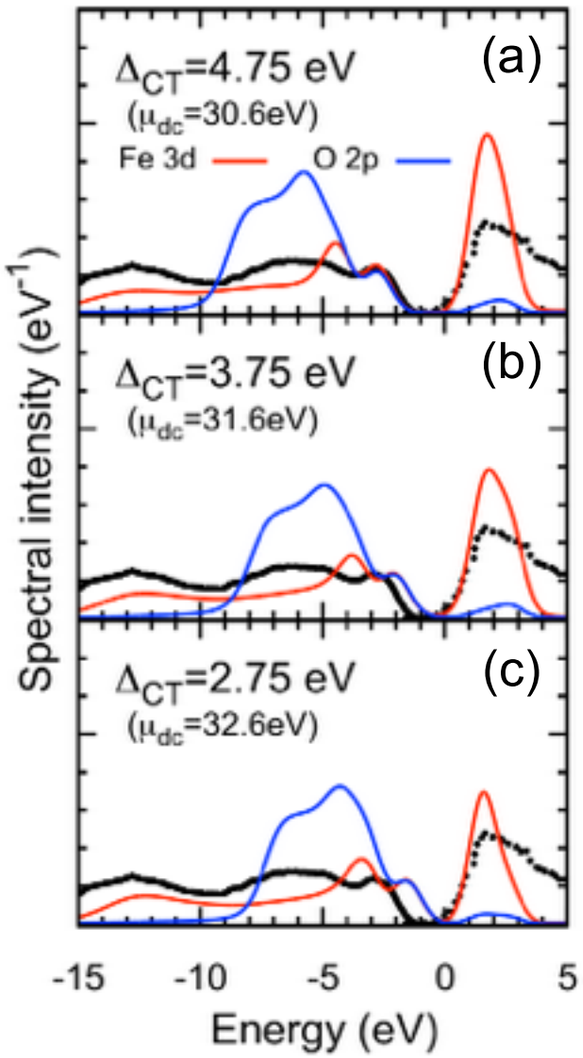

Fe L-edge XAS

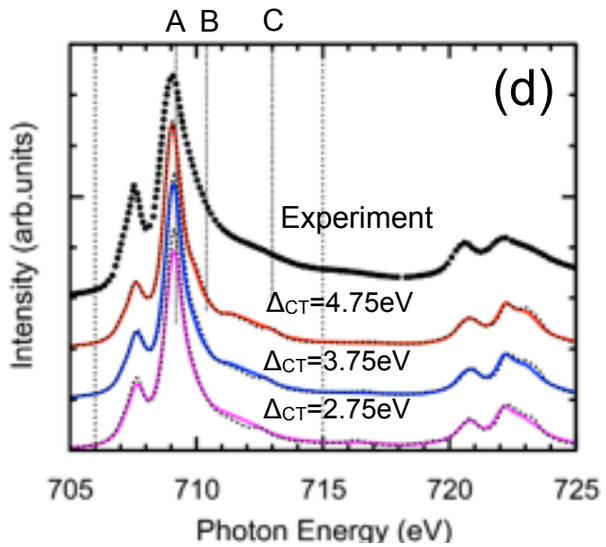

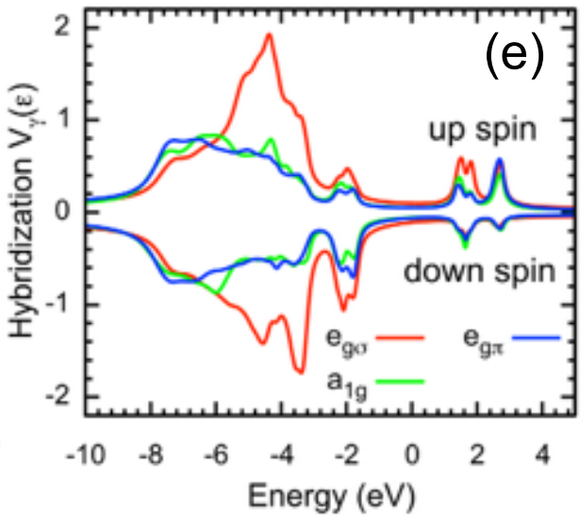

Fe L-edge RIXS

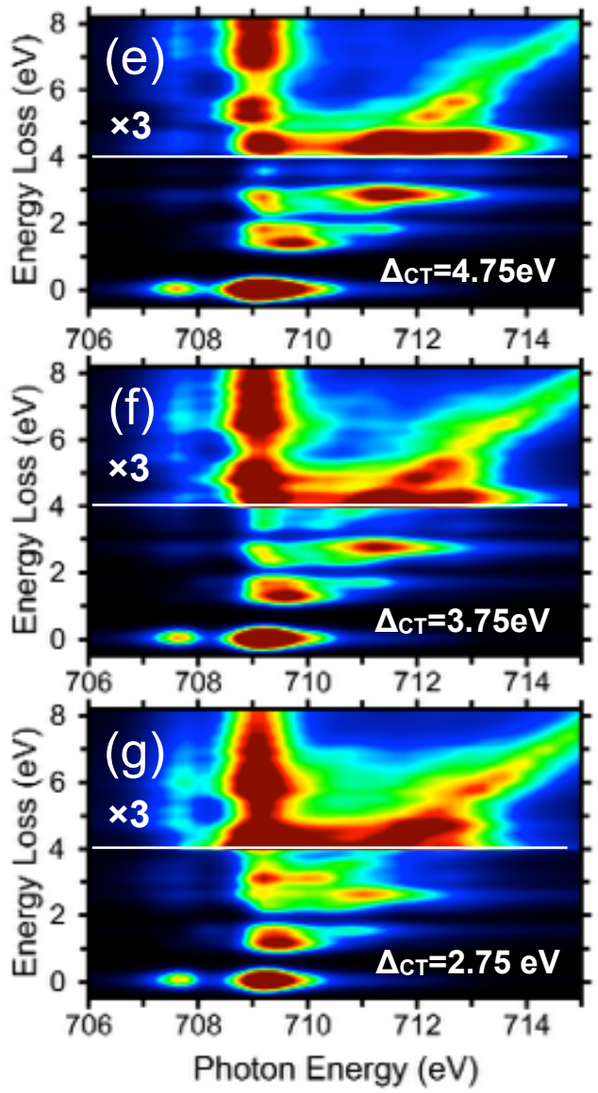

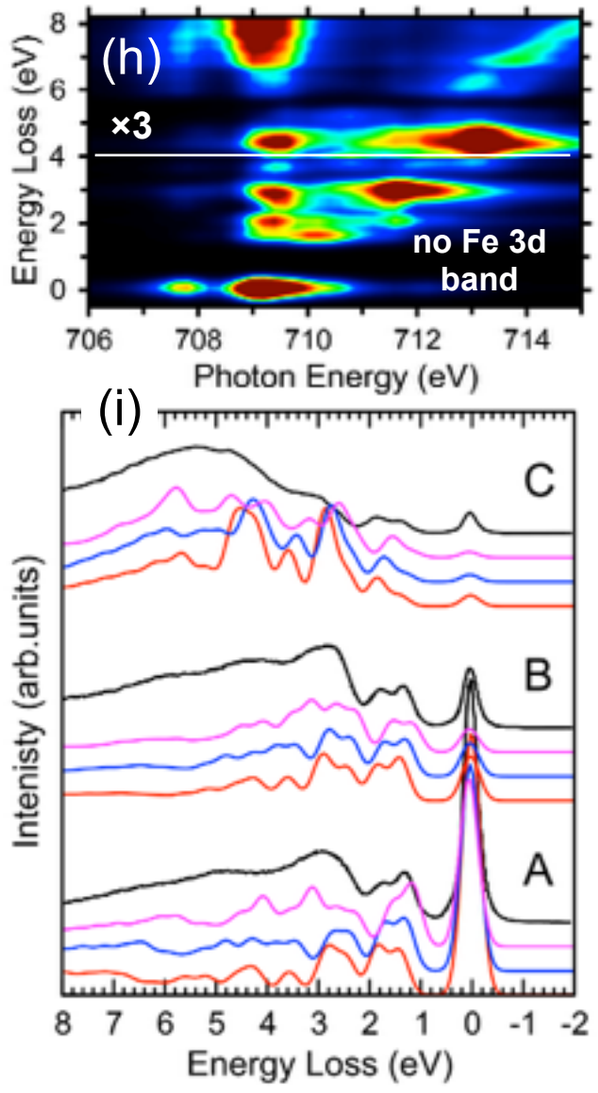

Good agreement with the experimental RIXS data

- **dd excitations (0~4eV) : multiplet, crystal field**
- **CT excitations (4~8eV) : local and nonlocal CT**
- **unbound excitations (4eV~) : fluorescence-like feature**

Experimental data

Valence PES/BIS : F. Ciccacci et al. PRB **44**, 10444 (1991)
R. J. Lad et al. PRB **39**, 13478 (1989)
L-edge XAS : M. L. Yang et al. PRB **80**, 014508 (2017)
L-edge XPS : M. Miedema et al. JESRP **203**, 8 (2015)
L-edge RIXS : J. Miyawaki et al. 96, 214420 (2017)

High-valence transition-metal ox

for Prague only

High-valence 3d transition-metal ?

22 Ti	23 V	24 Cr	25 Mn	26 Fe	27 Co	28 Ni	29 Cu
					4+	3+	

Small charge-transfer energy Δ

$$d^n \leftrightarrow d^{n+1}\underline{L}$$ (L : Ligand hole)

Oxygen 2p states play a role in low-energy physics

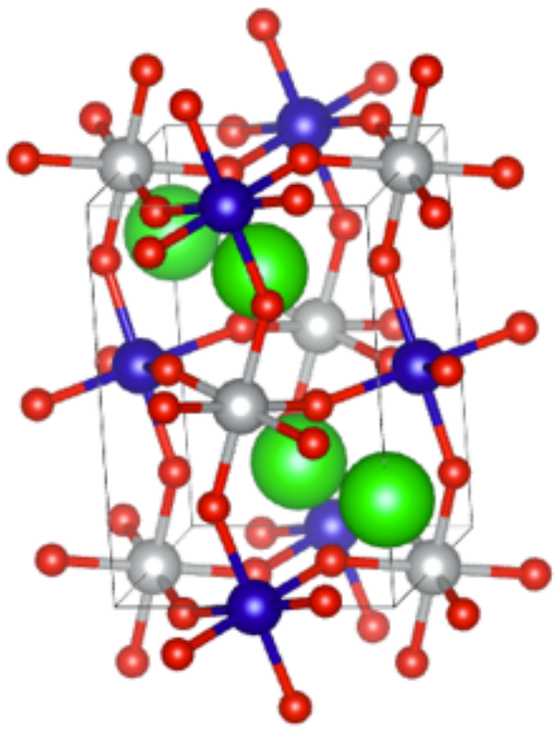

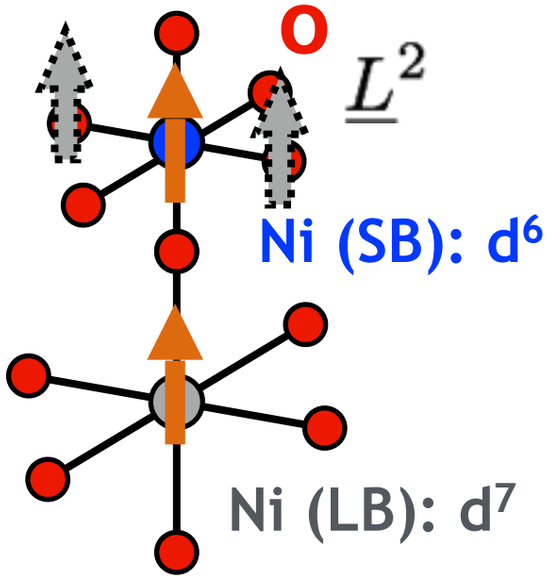

Rare-earth Nickelates : $RNiO_3$

C. Catalano et al. Rep. Prog. Phys. **81** (2018) 046501

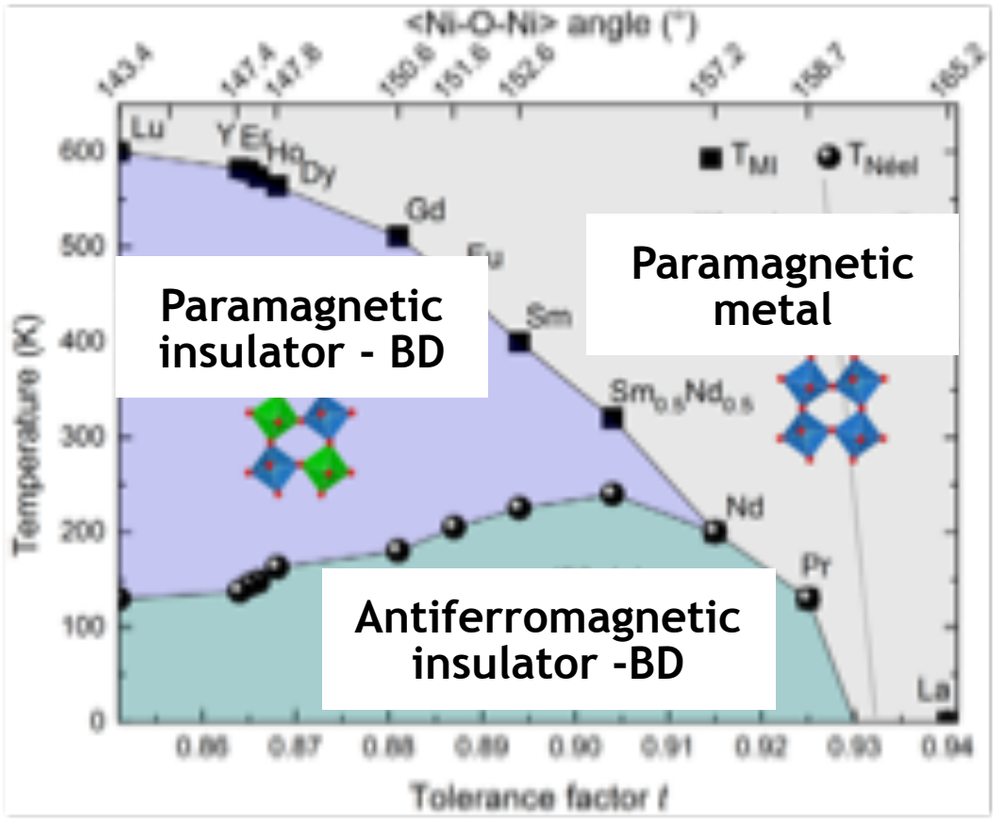

Charge-disproportionation

$$d^7 + d^7 \rightarrow d^6 + d^8$$
$$\rightarrow d^8\underline{L} + d^8\underline{L}$$
$$\rightarrow d^8\underline{L}^2 + d^8$$

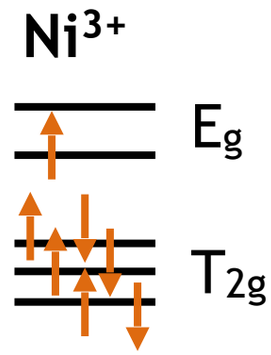

Short Ni-O bond Long Ni-O bond

High-valence transition-metal ox

for Prague only

Electronic + Structural + Ligand

H. Park et al. PRL **109**, 156402 (2012)

Electronic correlation

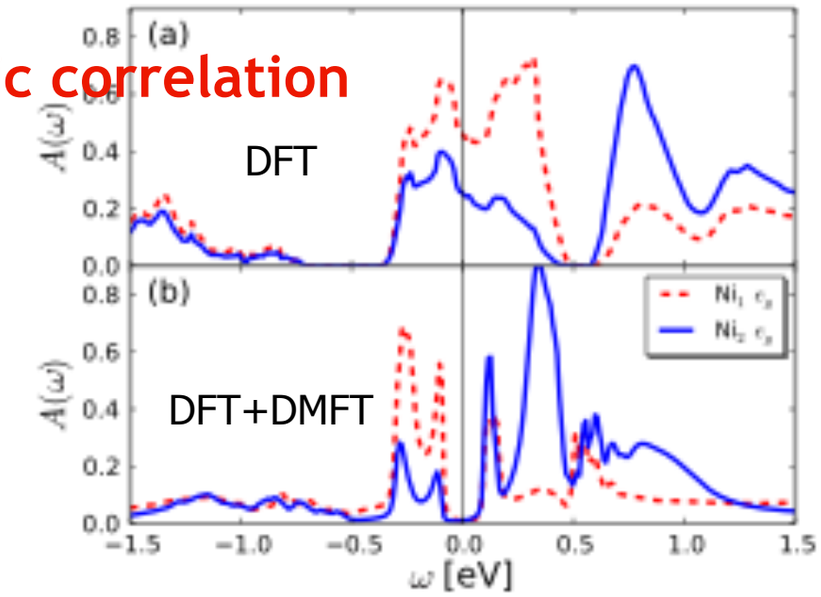

ARTICLE

DOI: 10.1038/s41467-017-01811-x OPEN

Structurally triggered metal-insulator transition in rare-earth nickelates

Nat.Commun. **7**, 13017 (2016)

Alain Mercy[1], Jordan Bieder[1,2], Jorge Íñiguez[3] & Philippe Ghosez[1]

Peierls-type instability

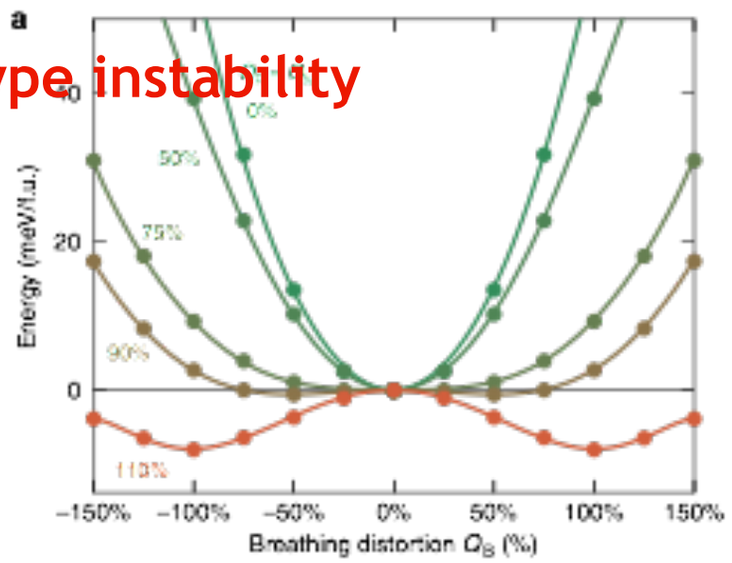

Rare-earth Nickelates : $RNiO_3$

C. Catalano et al. Rep. Prog. Phys. **81** (2018) 046501

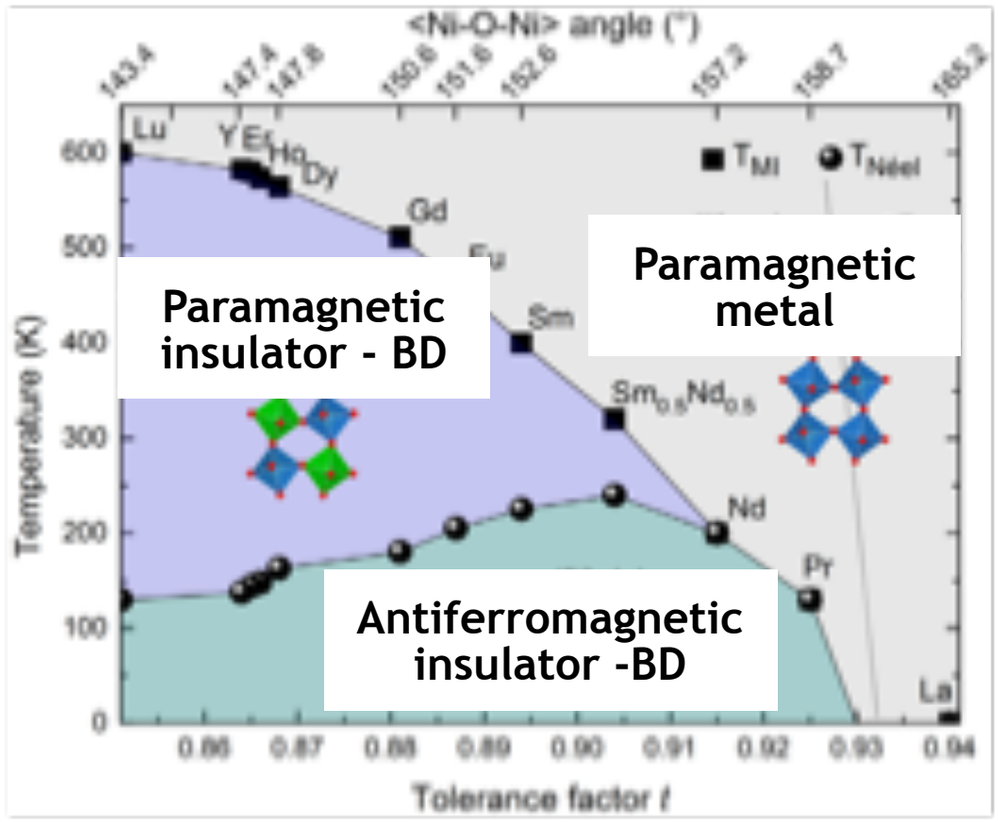

Charge-disproportionation

$$d^7 + d^7 \rightarrow d^6 + d^8$$
$$\rightarrow d^8\underline{L} + d^8\underline{L}$$
$$\rightarrow d^8\underline{L}^2 + d^8$$

Ni^{3+}

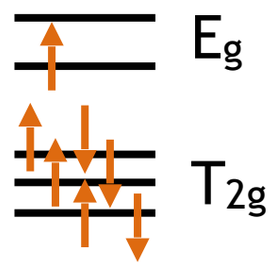

Short Ni-O bond **Long Ni-O bond**